Master's Thesis

Self-poling effect on Mn-doped $Pb(Mg_{1/3}Nb_{2/3})O_3$-$PbTiO_3$ single crystals synthesized by solid-state single crystal growth method

Geon-Ju Lee

Department of Materials Science and Engineering

Graduate School of UNIST

2020

Self-poling effect on

Mn-doped Pb(Mg$_{1/3}$Nb$_{2/3}$)O$_3$-PbTiO$_3$

single crystals synthesized

by solid-state single crystal growth method

Geon-Ju Lee

Department of Materials Science and Engineering

Graduate School of UNIST

Self-poling effect on

Mn-doped Pb(Mg$_{1/3}$Nb$_{2/3}$)O$_3$-PbTiO$_3$

single crystals synthesized

by solid-state single crystal growth method

A thesis

submitted to the Graduate School of UNIST

in partial fulfillment of the

requirements for the degree of

Master of Science

Geon-Ju Lee

12. 13. 2019. of submission

Approved by

_____

Advisor

Prof. Wook Jo

ii

Self-poling effect on

Mn-doped Pb(Mg$_{1/3}$Nb$_{2/3}$)O$_3$-PbTiO$_3$

single crystals synthesized

by solid-state single crystal growth method

Geon-Ju Lee

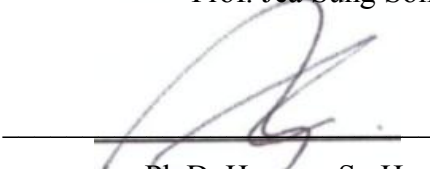This certifies that the thesis of Geon-Ju Lee is approved.

12. 13. 2019. of submission

_____

Advisor: Prof. Wook Jo

_____

Prof. Jea Sung Son

_____

Ph.D. Hyoung-Su Han

Table of contents

List of Figures

List of Tables

1. Introduction

Piezoelectric single crystal such as PZN-PT [Pb(Zn$_{1/3}$Nb$_{2/3}$)O$_3$-PbTiO$_3$] and PMN-PT [Pb(Mg$_{1/3}$-Nb$_{2/3}$)O$_3$-PbTiO$_3$] which have magnificent piezoelectric properties, have been used for various applications, e.g., sensors, transducers and actuators. For piezoelectric applications, ferroelectric materials are usually employed because of their high performance after poling process.

Poling process that forces ferroelectric domains to align; otherwise, randomly oriented, is essential in making a ferroelectric into a piezoelectric. It is typically performed at an elevated temperature by applying a certain amount of a unipolar electric field for some time since domain alignment is a time-dependent thermally activated process. However, induced piezoelectric properties generally disappear when ferroelectric material is heated up to Curie temperature (T$_c$) where aligned dipoles scatter. Because the synthesis of common ferroelectric materials is processed at high temperature, ferroelectric materials must be poled for piezoelectric application.

In this paper, ferroelectric PMN-PT single crystals with doping Mn for inducing self-poling effect will be discussed. The Mn-doped PMN-PT exhibits a high piezoelectric response without any poling process. Moreover, high piezoelectric properties are re-induced after heating above T$_C$ with self-poling on cooling process. The defect-dipoles which is caused by Mn ions generate internal bias fields (E$_i$) which give forces aligning dipoles of PMN-PT to have spontaneous polarization.

The Mn-PMN-PT crystal which is able to be self-poled has its own preferred poling direction. So opposite DC-poling can enhance piezoelectric and dielectric performances like AC-poling which is highly interested by ferroelectric single crystal society. The mechanism presented in this paper can offers a new perspective for enhancing the dielectric and piezoelectric properties of doped ferroelectric single crystals.

2. Theoretical review

2.1. Piezoelectrics

2.1.1. Classification of dielectric materials

Dielectric material is an electrical insulator that can be polarized in applied electric field, E. When electric field is applied to dielectric material, it responds with charge redistribution. The bound charge carriers stick in their unit cell, they are only arranged with same direction of applied electric field. The magnitude of the displacement (polarization density) proportionally increase with applied electric field given by **equation (1)**

$$P = \varepsilon_0 \varepsilon_r E \qquad\qquad (1)$$

Where ε_0, ε_r are the vacuum and the relative dielectric permittivity, respectively. The dielectric permittivity which means the measure for electrical energy stored can be measured by an applied voltage and the capacitance, C of the material. The capacitance is defined as followed **equation (2)** with A, the surface area and t, thickness of the material.

$$C = \varepsilon_0 \varepsilon_r \cdot \frac{A}{t} \qquad\qquad (2)$$

And there is electric-field induced strain effect which is given by **equation (3)** Where S is strain which is related to polarization by electrostrictive coefficient, Q.

$$S = Q \cdot P^2 \qquad\qquad (3)$$

Dielectric materials can be classified by several subgroups (See **Figure 1 and Figure 2**). For 21 non-centrosymmetric crystal classes have piezoelectric, pyroelectric and ferroelectric effects.
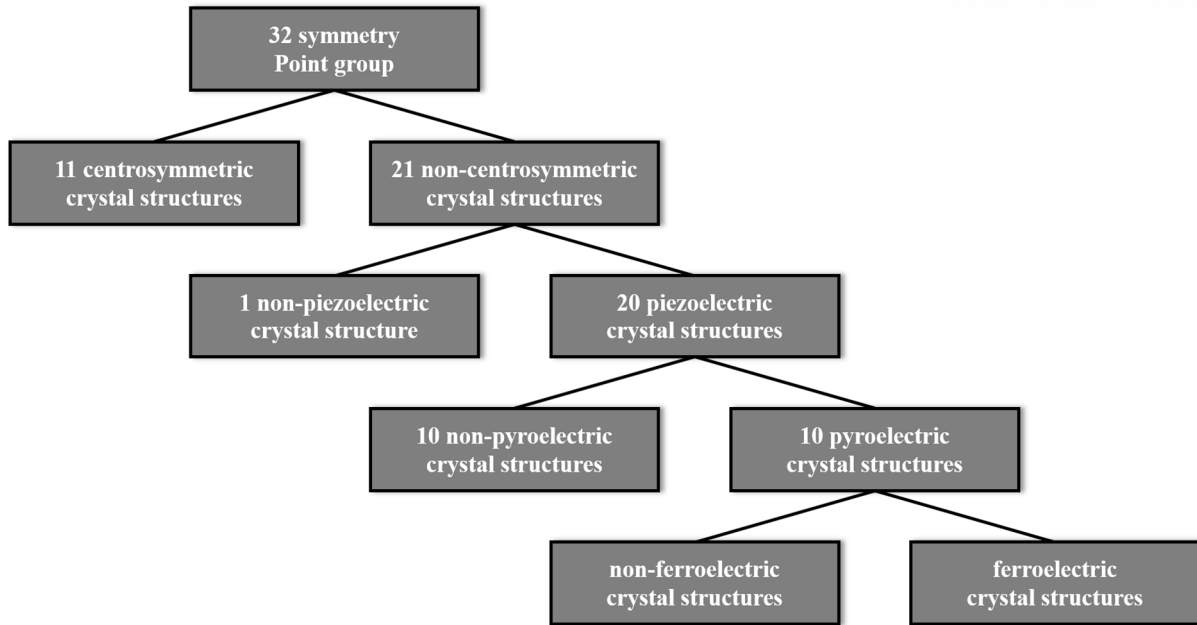
Figure 1. Classification of piezoelectric, pyroelectric and ferroelectric crystal based on the symmetry system
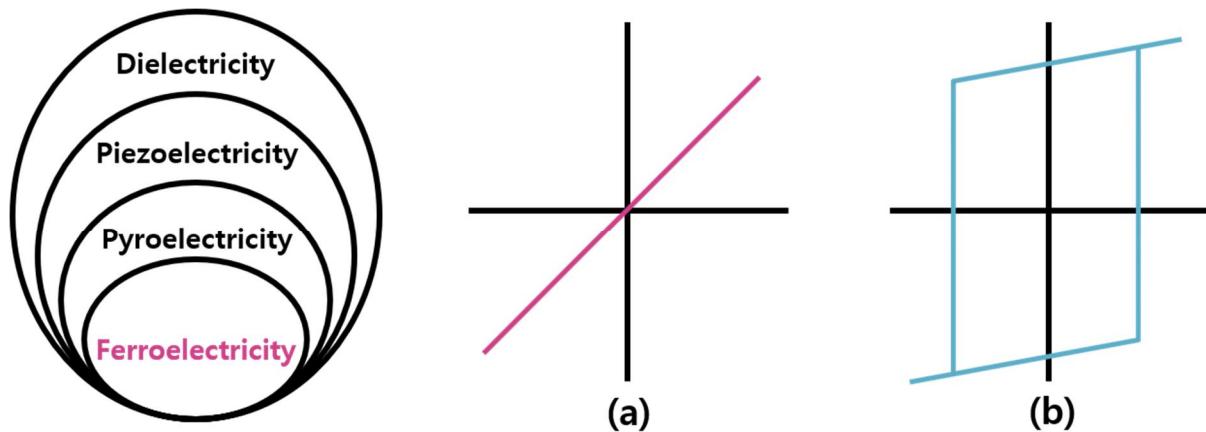
Figure 2. Scheme of the subgroups of dielectrics and the electric field E dependence of (a) dielectric electrostrictive and (b) ferroelectric polarization P

Piezoelectric effect

Piezoelectrics develop electrical polarization when mechanical stress is applied. 20 crystal structures in the 21 non-centrosymmetric classes show this effect. The piezoelectric relation with polarization(P), stress (σ) and the piezoelectric coefficient(d_{ijk}, tensorial quantity) is defined as **equation (4).**

3

$$P_i = d_{ijk}\sigma_{jk} \qquad\qquad \textbf{(4)}$$

The inverse piezoelectric effect, which is the production of strain S by applied electric field E, is defined by **equation (5)**.

$$S_{jk} = d_{ijk}E_i \qquad\qquad \textbf{(5)}$$

Pyroelectric effect

Pyroelectrics are a subgroup of piezoelectric materials whose spontaneous polarization, P_s shows temperature dependent. The dependence of polarization on temperature can be described by **equation (6)** with the pyroelectric coefficient γ .

$$P_i^s = \gamma_i\Delta T \qquad\qquad \textbf{(6)}$$

Ferroelectric effect

Ferroelectric material is a subgroup of pyroelectric material with two or more orientational states of the spontaneous polarization without electric field which can be reversed by the external electric field. More details about ferroelectric material will be dealt with next chapter.

2.1.2. The structure of ferroelectric materials

At high temperature, all ferroelectric materials have cubic phase where only induced polarization and electrostriction exists. In this paraelectric phase, polarization is directly proportional to the electric field. There is no spontaneous polarization, the material cannot have extrinsic polarization.

Most commonly used ferroelectrics, such as barium titanate ($BaTiO_3$), potassium niobate ($KNbO_3$) and lead titanate ($PbTiO_3$) have a perovskite crystal structure (see **Figure 3**). [1] ABO_3 is the general formula of perovskites. It has a cubic unit-cell in its high temperature paraelectric phase and several polymorphs at lower temperatures (see **Figure 3**). The large A-atoms occupy the cube corners, the smaller B-atoms form the unit cell center and the oxygens are found at the face centers. The B atoms have a coordination number of 6 surrounded by oxygen octahedral, the A-atoms have a coordination number of 12.
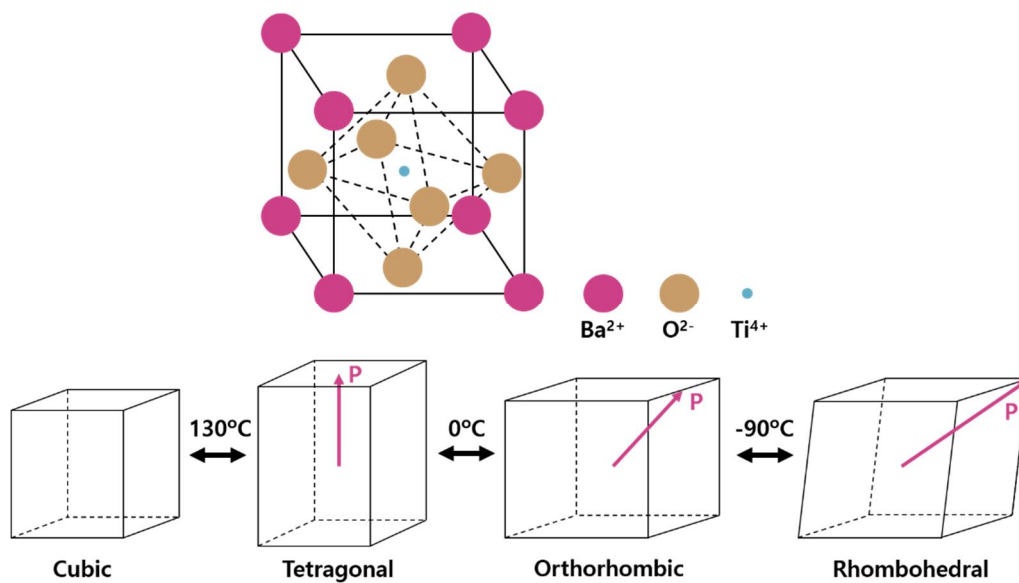
Figure 3. Perovskite structure of the ferroelectric $BaTiO_3$ in its cubic paraelectric phase above the Curie point Tc of 130°C. The tetragonal, orthorhombic and rhombohedral ferroelectric polymorphs and their respective directions of polarization P are sketched.[2]

2.1.3. Phase transition of ferroelectric materials and Curie point
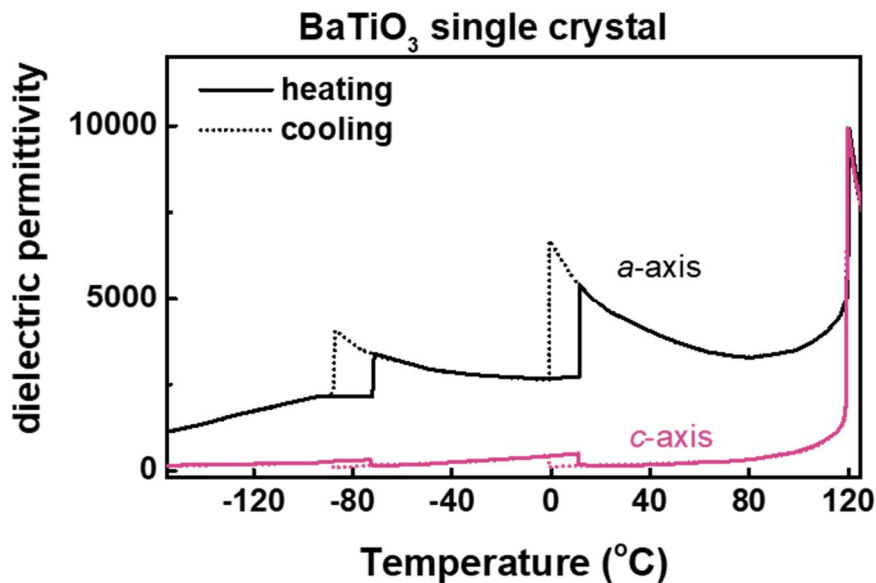
Figure 4. Dielectric permittivity for a-axis and c-axis of $BaTiO_3$ single crystal as function of Temperature.**[3]**

The ferroelectric material undergoes several structural phase transitions during heating or cooling. $BaTiO_3$ has three phase transitions in the temperature range from -90 °C to 130 °C . **Figure 3** and **Figure 4** shows the structure and dielectric permittivity of $BaTiO_3$ upon phase transition. The rhombohedral, orthorhombic and tetragonal $BaTiO_3$ has ferroelectricity, while the cubic phase is paraelectric.**[4]**

The Curie temperature (T_c) of ferroelectricity means the temperature where spontaneous polarization of ferroelectric materials decreases to zero and the phase transition point from ferroelectric to paraelectric. Spontaneous polarization of ferroelectric materials decreases with increasing temperature up to the phase transition temperature, T_c, where the polarization disappears continuously (2nd order phase transition) or more often discontinuously (1st order phase transition) (**Figure 5** (b), (e) respectively).**[1]**
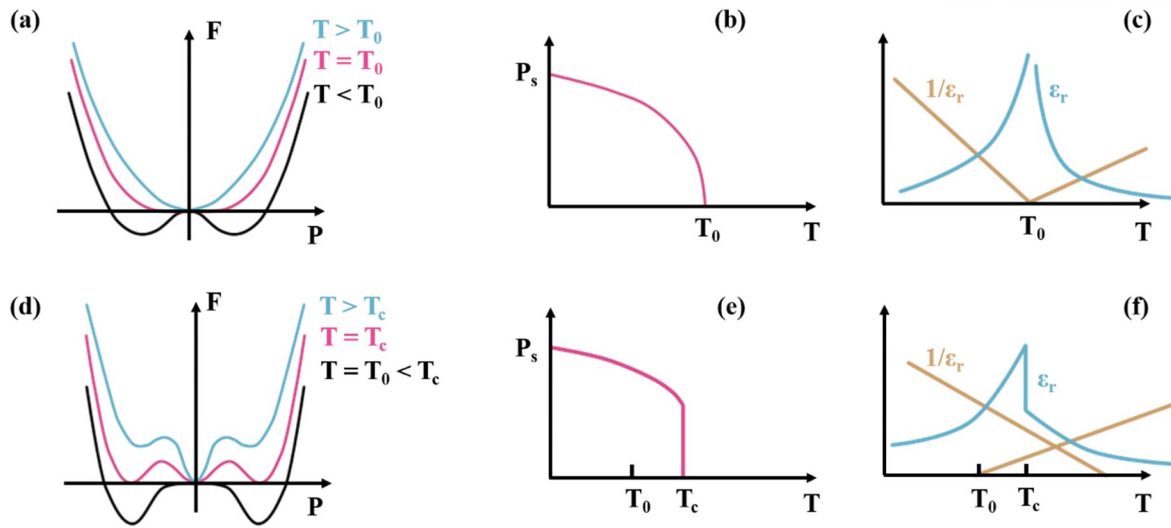
Figure 5. Features of (a-c) second order and (d-f) first order phase transition. (a, d) Free energy as a function of polarization(b, e). Spontaneous polarization Ps as a function of temperature(c, f).**[5]**

The dielectric permittivity and its inverse, following the Curie-Weiss law given by **equation 7**. This structural phase transition is accompanied by a diverging differential dielectric permittivity, which can be described with the Curie-Weiss law

$$\varepsilon_r = \frac{C}{(T - T_0)} \qquad (7)$$

where C is the Curie-Weiss constant and T_0 stands for the Curie-Weiss temperature, which is defined as the x-axis intercept of the linear portion of the plot of $1/\varepsilon_r$ versus T above the Curie point (see **Figure 5** c, f).**[5]**

2.1.4. Ferroelectric domains and their switching mechanism

Ferroelectric materials below T_c without an external field have at least two equivalent directions of spontaneous polarization. Different regions of the crystal polarize in these different directions. The uniform polarizations make their own area, which is called a domain. The domain structure usually results in zero net polarization of the material. Domain boundaries are arranged so that the dipole moments of individual domains meet at either 180°

or 90° in tetragonal structure and 71° or 109° in rhombohedral crystal symmetry. This twinning of domains reduces the overall free energy in comparison to a single domain configuration. Because the domain boundaries (domain walls) also store energy, the actual domain structure is a result of the balance of energy increase due to domain wall creation and energy decrease due to reduction of the depolarization field.[6]

Before Poling, $P_r = 0$ **After Poling, $P_r \neq 0$**
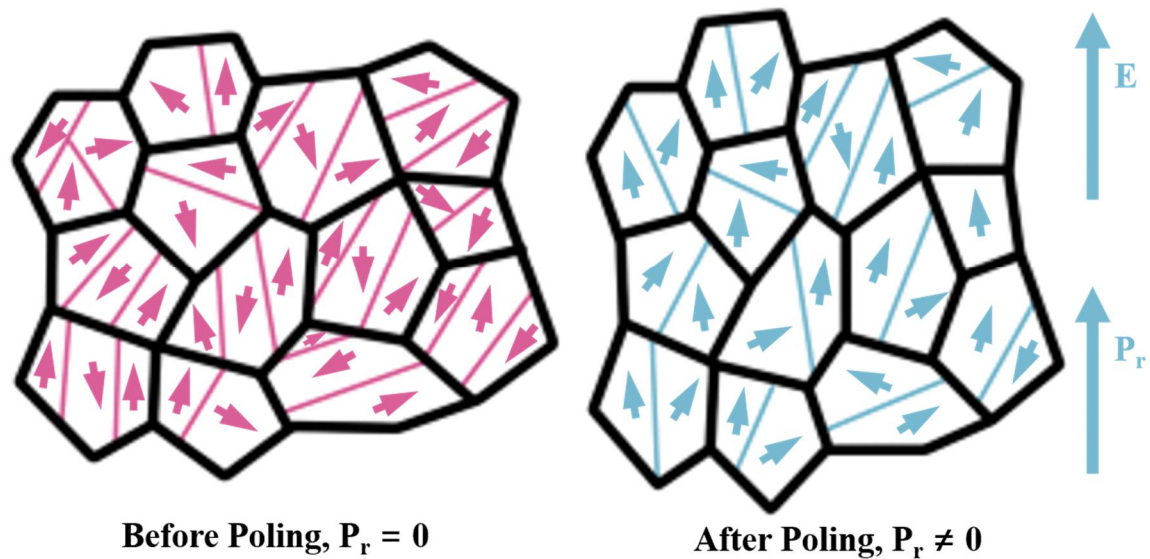
Figure 6. Sketch of a random orientation state in a ferroelectric ceramic before and after poling.[7] Before poling the macroscopic remanent polarization P_r is zero. After poling, the domains are preferentially aligned with the electric field E. This results in non-zero remanent polarization P_r and strain S_r.

When ferroelectric material poled with external field, the crystal lattice changes with small deformations. These polarization and strain changes are referred to as an intrinsic effect. Intrinsic changes of polarization and strain are reversible and do not contribute to hysteresis.[6] When external electric field continuedly increase, domain also coalesce to grow into bigger with favored orientations.

Domain wall motion results in a deformation from a change of direction of polarization in the volume which is swept by the wall. Work from domain wall is done during this process. This extrinsic effect (Domain wall motion) contributes to the hysteretic behavior. In **Figure 6** describes poling process. Poled material shows macroscopic remanent polarization and strain

after removal of the external field. The degree of poling is related to the number of possible poling directions and their alignment with the external field.[4]
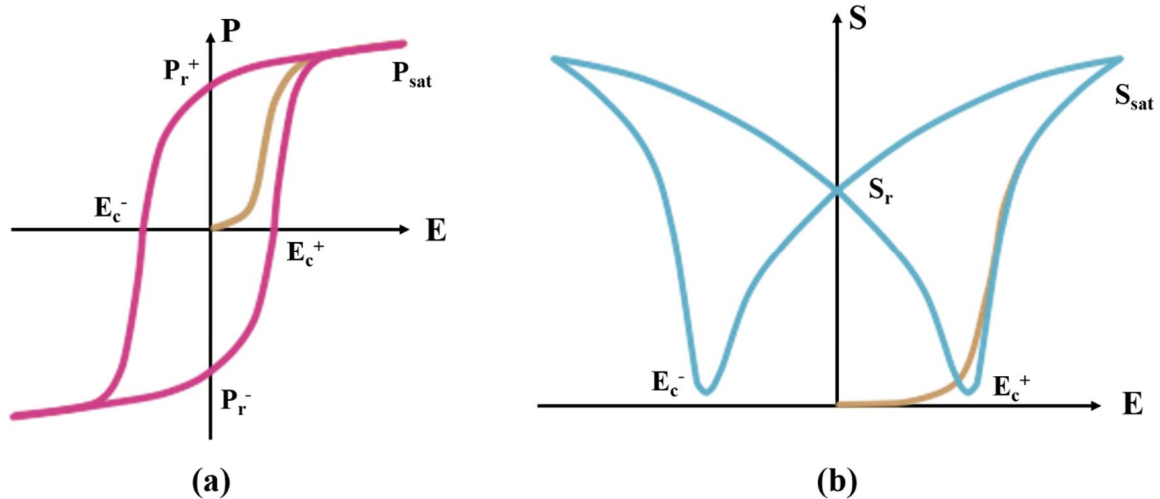
Figure 7. **(a)** Ferroelectric polarization hysteresis loop. **(b)** Strain hysteresis loop showing the characteristic butterfly curve.

A typical polarization - electric field curve (PE curve) is shown in **Figure 7 (a).** When electric field is applied to an unpoled ferroelectric material, the randomly oriented domains are successively oriented with the direction of electric field. Increasing the electric field leads to a saturation polarization P_{sat} where most dipoles are aligned with direction of electric field. When the polarization increases linearly with electric field because of polarization extension, the degree of polarization has reached its maximum. Although the external field is lowered, direction of dipoles is not changed and leave a remanent polarization, P_r when electric field gets zero. The linear extrapolation of the saturation curve back to zero field represents the spontaneous polarization P_s. When a opposite direction field is applied, the domains align in the new field direction and the polarization reaches zero at the coercive field, E_c and repeat same process.[7]

Like the PE curve, strain under an alternating electric field has hysteresis because of polarization switching. The so-called butterfly-loop is shown in **Figure 7 (b)**. Total strain of ferroelectric material is the sum of an intrinsic contribution, which means the unit cell extension, and an extrinsic contribution, due to domain wall motion. The latter changes the relative

9

number of domains of one orientation in favor of an orientation which is better adopted to the local stress and electric field state. Ferroelectric ceramics usually contain non-180° domains, which is switched in direction of the field and contribute significantly to the strain of the sample.[6]

2.1.5. Dynamics of Ferroelectric systems
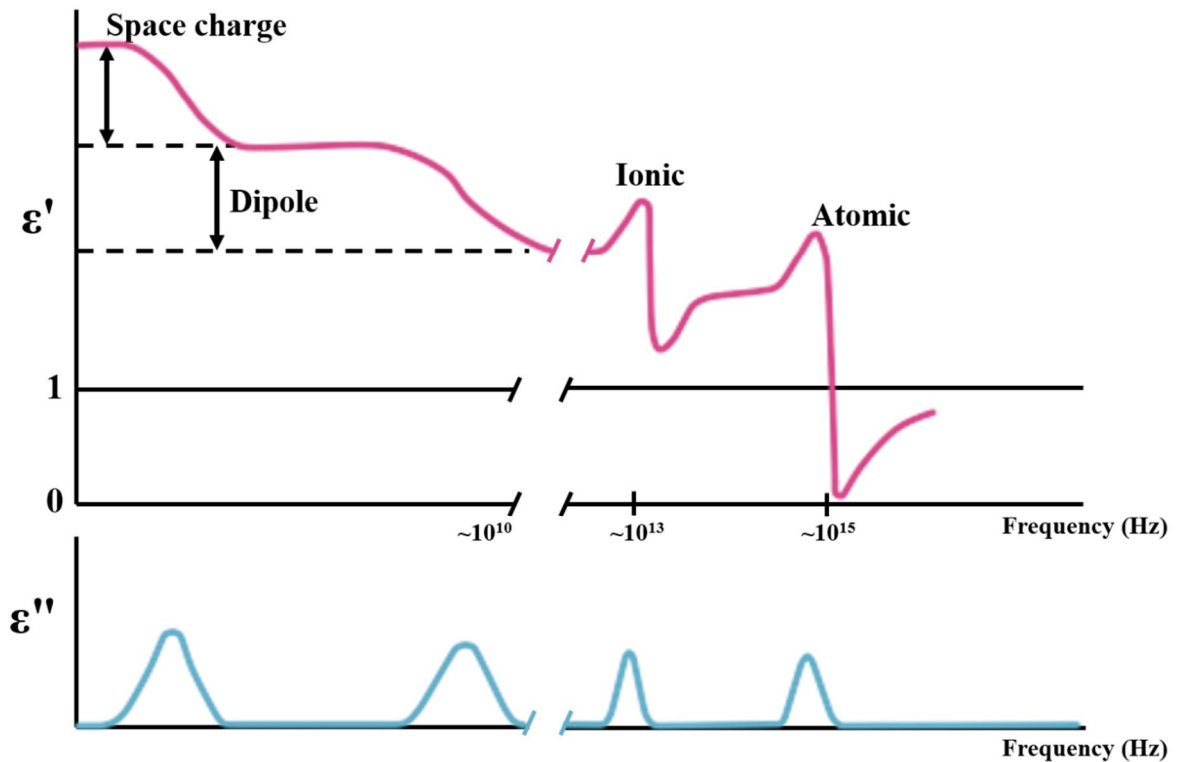
Figure 8. Variation of the complex dielectric permittivity with frequency.[2]

The polarization **P** is the result of contribution of several polarization mechanisms with different relaxation frequencies. In general dielectrics, the macroscopic polarization is the sums for each polarization of atoms, ions, dipoles and space charge. This relation can be described by **equation (8)**.

$$\varepsilon_{total} = \varepsilon_{atomic} + \varepsilon_{ion} + \varepsilon_{dipole} + \varepsilon_{Spacecharge} \tag{8}$$

Atomic polarization, which means the deformation of the electron cloud around an atomic

10

nucleus, has the fastest response time and adds to macroscopic polarization up to frequencies of 10^{15} Hz. **Ionic displacements** are the most important contribution to polarization in ferroelectric ceramics. Because mass of ions is higher than that of electrons, ionic mechanism responds more slowly (frequencies of 10^{13} Hz).**[2]** Dipolar polarization and space charge polarization which involves a limited transport of charge carriers, respond at much lower frequencies. In other words, depending on the frequency of the applied alternating field, different polarization mechanisms can be activated. The dielectric and piezoelectric response is therefore highly frequency dependent. Because charges have inertia, the polarization does not occur instantaneously in response to an alternating field and dielectric permittivity is a complex quantity with a real ε' and an imaginary part ε''. **Figure 8** shows variation of the complex dielectric permittivity with frequency.**[2]**

2.2. Piezoelectric single crystal

2.2.1. Introduction

Piezoelectric ceramics have been modified for lower production costs and easier production methods because of its lower properties compared to piezoelectric single crystals. So, many of the industries (such as piezoelectric actuators, ultrasonic transducers, medical devices and sonar) that demand high performances use piezoelectric single crystals instead of ceramics. After development of $PbZrO_3$-$PbTiO_3$ (PZT) ceramics, there is no significant increase of properties for piezoelectric ceramics. But piezoelectric single crystal has much higher dielectric coefficient(d_{33}) and electromechanical coupling factor(k_{33}) than piezoceramics. **Table 1** shows the comparison of PZT ceramics (polycrystal) and PMN-PT single crystals. For d_{31} and k_{31}, PMN-PT single crystal has eight and two times higher respectively compared to PZT-5H ceramics.

	d_{33} [pC/N] (k_{33})	d_{31} (k_{31})	d_{15} (k_{15})	d_{36} (k_{36})
PMN-PT Single crystal	$1,500 \sim 2,500$ ($k_{33} > 0.9$)	$1,000 \sim 2,000$ ($k_{31} > 0.85$)	$4,000 \sim 6,000$ ($k_{15} > 0.95$)	$2,000 \sim 2,500$ ($k_{36} > 0.9$)
PZT-5H ceramics	600 ($k_{33} \sim 0.75$)	250 ($k_{31} \sim 0.4$)	750 ($k_{15} \sim 0.7$)	0 0

Table 1. Comparison of PZT ceramics (polycrystal) and PMN-PT single crystals.[8]

Table 2 illustrates the properties of all generation piezoelectric single crystals. It was around 1980s when the research about relaxor-$PbTiO_3$ piezoelectric single crystals because of its outstanding properties. In 1980s, Kuwata in Tokyo Institute of Technology developed $Pb(Zn_{1/3}Nb_{2/3})O_3$-$PbTiO_3$ (PZN-PT) single crystal[9] and Tom Shrout in Pennsylvania State University reported synthesis of $Pb(Mg_{1/3}Nb_{2/3})O_3$-$PbTiO_3$ (PMN-PT) single crystals.[10] These two relaxor-$PbTiO_3$ piezoelectric single crystals is called the first-generation single crystals. But depolarizing temperature of these crystals is too low to use for applications despite high electromechanical coupling factor of PZN-PT and PMN-PT single crystals. So, second generation piezoelectric crystal, such as $Pb(In_{1/2}Nb_{1/2})O_3$-$Pb(Mg_{1/3}Nb_{2/3})O_3$-$PbTiO_3$ (PIN-

PMN-PT) and $Pb(Mg_{1/3}Nb_{2/3})O_3$-$PbTiO_3$-$PbZrO_3$ (PMN-PZT), was fabricated for extending operation range of temperature and coercive field. Then third generation piezoelectric single crystals like Donor/Acceptor Modified PMN-PT and PMN-PZT have been developed to get high mechanical quality factor and more outstanding piezoelectric performances.

	Compositions	Dielectric and Piezoelectric Properties
Generation 1	PMN-PT PZN-PT	$T_{RT} < 100°C$; $E_C < 3$ kV/cm; $k_{33} > 0.9$; $d_{33} > 1,500$ pC/N
Generation 2	PIN-PMN-PT PMN-PZT	$T_{RT} > 100°C$; $E_C > 3$ kV/cm; $k_{33} > 0.9$; $d_{33} > 1,500$ pC/N
Generation 3	Acceptor (Mn, ect.) Modified PMN-PT PMN-PZT	$T_{RT} > 100°C$; $E_C > 3$ kV/cm; $k_{33} > 0.9$; $d_{33} > 1,500$ pC/N (Very High d_{33} or Q_m Optimized by Donor/Acceptor)

Table 2. Three generations of high performance piezoelectric single crystals.[8]

2.2.2. Dopant engineering for Piezoelectric single crystal

As the study of $Pb(Zr_{1/2}Ti_{1/2})O_3$ ceramics has shown, the piezoelectric properties are improved by adding donor or acceptor dopants. Therefore, currently commercialized PZT ceramics are usually doped with donor or acceptor dopants. The technique that uses dopants to change the piezoelectric properties is called "Dopant engineering". For synthesizing general ceramics, the processes using dopants are not quite difficult to disperse dopants in ceramic lattice. But in case of synthesis of single crystal, even 1% of dopants greatly affect to growth condition of crystals and the segregation of dopant is also severe. So there have been many studies for synthesizing doped crystal and recently, Mn-doped PMN-PZT has been synthesized and the mechanical quality factor Q_m and coercive electric field (E_C) of crystal increased compared to pure PMN-PZT, a result of formation of internal bias field. Although the dielectric permittivity of doped crystal decreased as hard piezoelectric ceramics, electromechanical coupling factor (k_{33}) remained about 0.9 unlike general case of inverse proportional with Q_m. [11]
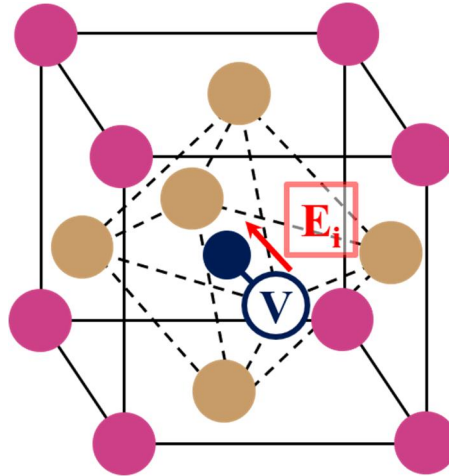
Figure 9. Formation of internal bias field in acceptor-doped perovskite materials.

Figure 9 shows the internal bias field of acceptor-doped perovskite lattice. The acceptor dopant cations are substituted into the lattice point, oxygen vacancies are created for maintaining overall charge balance. Because of relative charge of these defects, they can make dipoles, we called defect dipole, and these dipoles makes the internal bias field.

2.2.3. Other modifications of piezoelectric single crystals

Although piezoelectric single crystals show outstanding performances, commercialization of single crystals such as PZN-PT and PMN-PT still faces a lot of obstacles. In addition to usage temperature and electric field of piezoelectric single crystals, reproducibility of their composition and properties and high cost from the lack of usable volume of synthesized single crystal which has full material properties for device design and purposes is another major problem. **Figure 10** compares the piezoelectric coefficient(d_{33}) variation of PMN-PT single crystal synthesized by Bridgman method with the compositional distribution measured by EPMA, which shows that the MPB zone (Ti concentration of 31-35%) has only 20% of the total boule volume.[12]
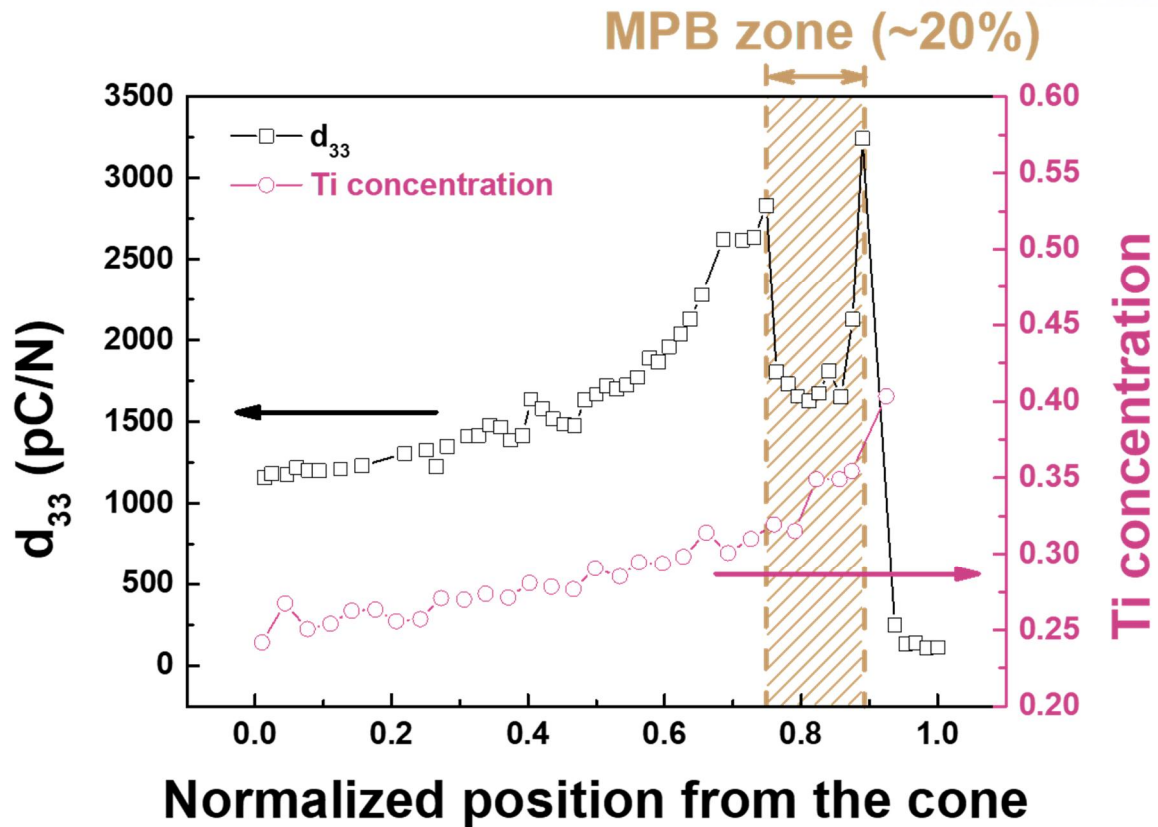
Figure 10. Comparison of piezoelectric coefficient variation with Ti concentration distribution along the same PMN-PT boule.[12]

The relaxor-PT single crystals for higher usage temperature and coercive field have been being studied including crystal doping. Staying low PT contents, the growth and characterization of PMN-PT and PZN-PT doped with Fe, Co, Mn etc. have recently been attempted. Some interesting results in these studies show that doping can be used to advantage to change the Curie and rhombohedral to tetragonal phase transition temperatures[13]–[16] and to give a hardening effect to the crystal, such as increasing the coercive field, mechanical quality factor and vibration velocity.[13]–[18] Doping has also been used to alter the photo-reflective, pyroelectric and photovoltaic properties of piezoelectric single crystals.[19]–[21] Because there are conflicting results presented by various studies, doping effects on the dielectric permittivity and piezoelectric coefficients of piezoelectric single crystals are unclear. [13], [15], [16], [18]
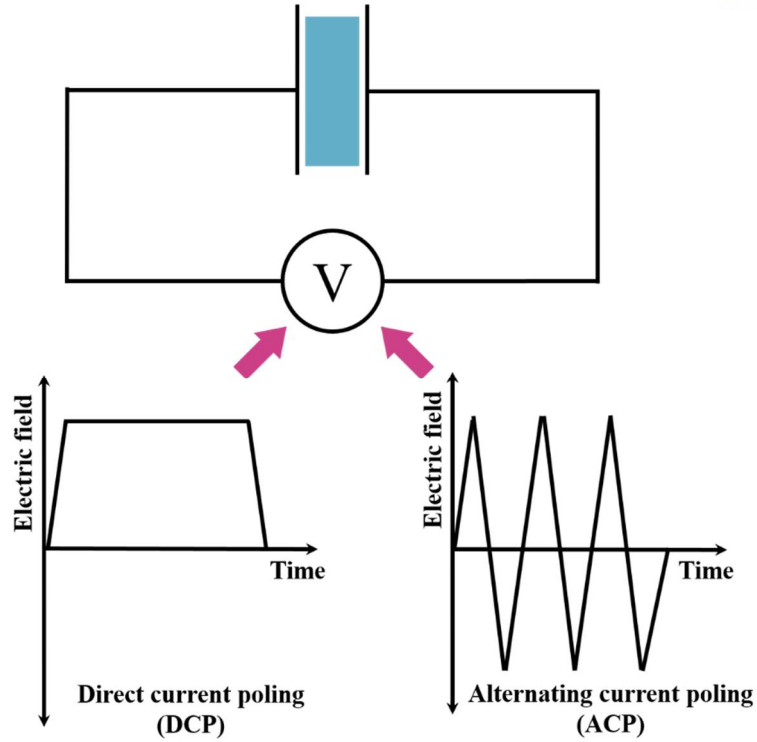
Figure 11. Comparison of Direct current poling (DCP) and Alternating current poling(ACP)

Alternating Current Poling(ACP) treatment for enhancing the dielectric constants and piezoelectric coefficients has recently been spotlighted. **Figure 11** describes the comparison of Direct current poling (DCP) and Alternating current poling(ACP). Yamashita and Yamamoto firstly reported the domain size engineering by alternating current poling process can be cost-effective method to enhance the piezoelectric properties of PMN-xPT single crystals.[22] And Xu et al. later proposed that PMN-25PT, which was not used due to its low properties, improved to the PMN-30PT level near MPB through ACP with 40% promotion for piezoelectric coefficient.[23] And Chang et al. reported that there is no significant difference in the aging rate of AC poled PMN-30PT single crystals.[24]
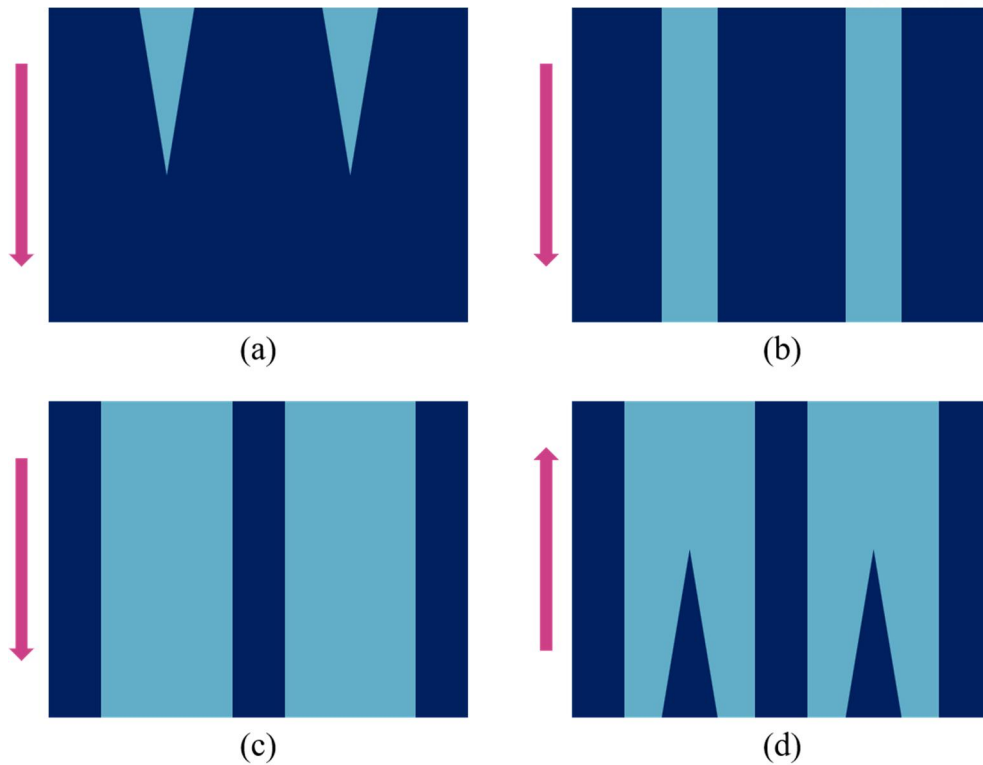
Figure 12. The main stages of the domain switching during polarization reversal in ferroelectrics

The possible reason for the ACP is described in **Figure 12** which shows the formations of nano-domains, observed by piezoelectric Force Microscopy. First (a) a new domain is created and (b) the domain is grown in the same direction as the field. (c) and increase the volume of the domain. (d) The same thing is then repeated in the opposite direction. When nano-domains are created, domain walls are relatively instable because of the formations of charged domain walls. However, the origins of ACP are still unclear.

3. Experimental procedure

3.1. Sample preparation

3.1.1. PMN-PT single crystal synthesized by Solid State Crystal Growth(SSCG) method

The pure $0.70Pb(Mg_{1/3}Nb_{2/3})O_3$-$0.30PbTiO_3$ (PMN-30PT) and Mn-doped PMN-30PT single crystals with (001) orientation were prepared by a solid-state single crystal growth (SSCG) technique at Ceracomp Co. Ltd. (Cheonan, Korea). After polished, gold electrodes are decomposed on the (001) planes of the single crystals for measuring electrical properties.

3.2. Characterization Techniques

3.2.1. X-ray diffraction

To confirm a crystallographic structure of single crystals, X-ray diffraction was performed with a CuK_α radiation (XRD: SmartLab, Rigaku, Tokyo, Japan). The 2θ-range from 20° to 80° was scanned for powdered sample.

3.2.2. X-ray photoelectron spectroscopy

The valence states of Mn ions were confirmed by X-ray photoelectron spectroscopy (XPS: K-alpha, ThermoFisher, Waltham, Massachusetts, USA). The XPS spectrum was scanned in the binding energy range of 630-660 eV.

3.2.3. Electric field induced properties of ferroelectric materials

To investigate electric field–polarization (P(E) hysteresis curve) and the temperature dependence of the polarization, coercive field(E_c) and internal bias field(E_i), the piezoelectric evaluation system was used (aixACCT aixPES, Aachen, Germany). The system consists of the TF Analyzer 2000, a voltage amplifier (Trek 610E, 10kV). The P(E) hysteresis curve was performed in condition that frequency is 1Hz and electric field is up to 1.5kV/mm. The temperature dependence of polarization was investigated in the range of 20°C and 200°C.

3.2.4. Temperature dependence of impedance spectroscopy

For investigating phase transition and temperature-dependence of dielectric permittivity and dielectric loss, impedance/gain phase analyzer (HP 4194A, Hewlett-Packard Company, Palo Alto, CA) in conjunction with a customized furnace with the oscillation voltage level at 1V, frequency range from 1kHz to 1MHz. The customized furnace is described in **Figure 13**.
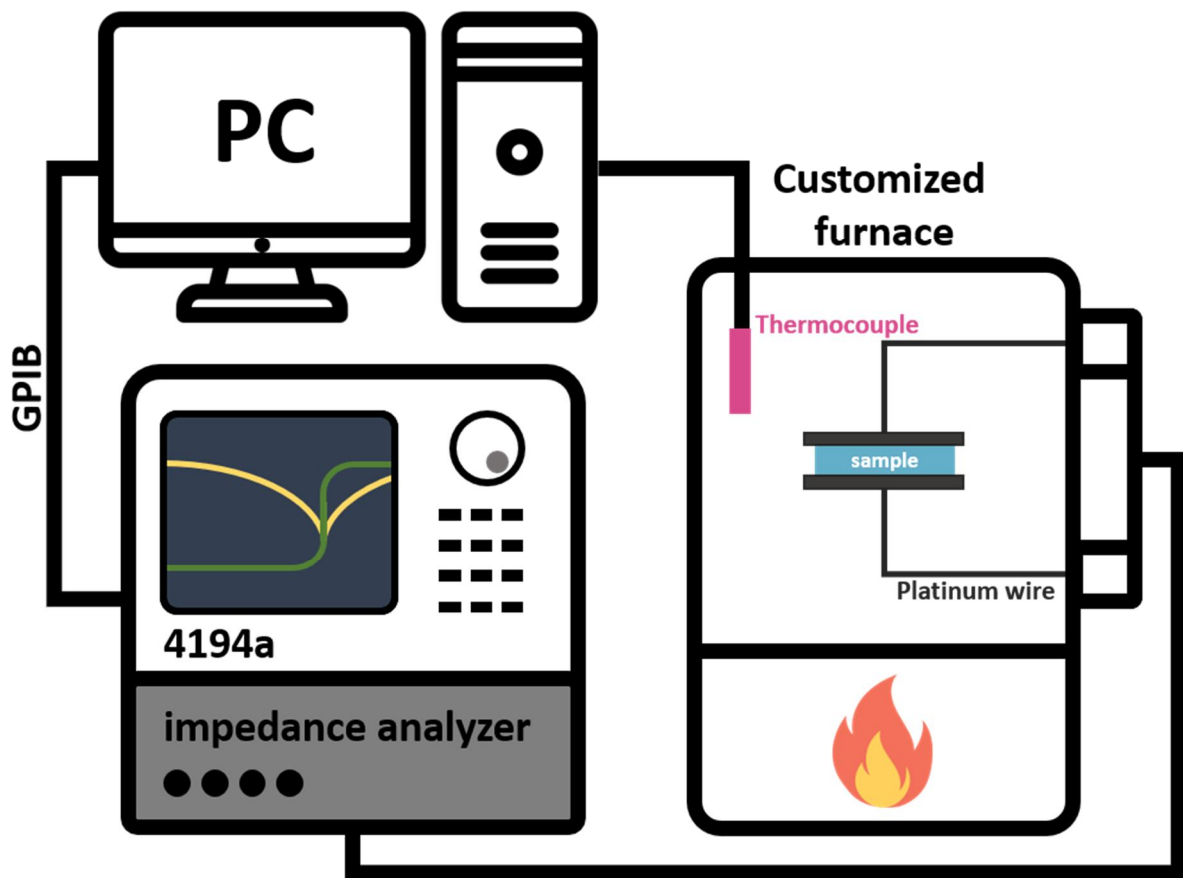
Figure 13. System scheme for measurement of temperature-dependence of impedance spectroscopy.

Samples were placed into a customized furnace, and the temperature was recorded with temperature measuring system (USB-TC-01, National Instruments, USA) which consists of a thermocouple directly next to the sample.

19

3.2.5. Thermally Stimulated Depolarization Current

For investigating depolarization current, thermally stimulated depolarization current (TSDC) measurement was performed. Currents were measured during heating with a picoammeter (picoammeter/voltage source 487, Keithley, Cleveland, OH) at the absence of an electric field. Samples were placed into a customized furnace, and the temperature was recorded with temperature measuring system (USB-TC-01, National Instruments, USA) which consists of a thermocouple directly next to the sample. **Figure 14** describes poling system and TSDC system with electric field, temperature and current profile in poling process and TSDC measurement.
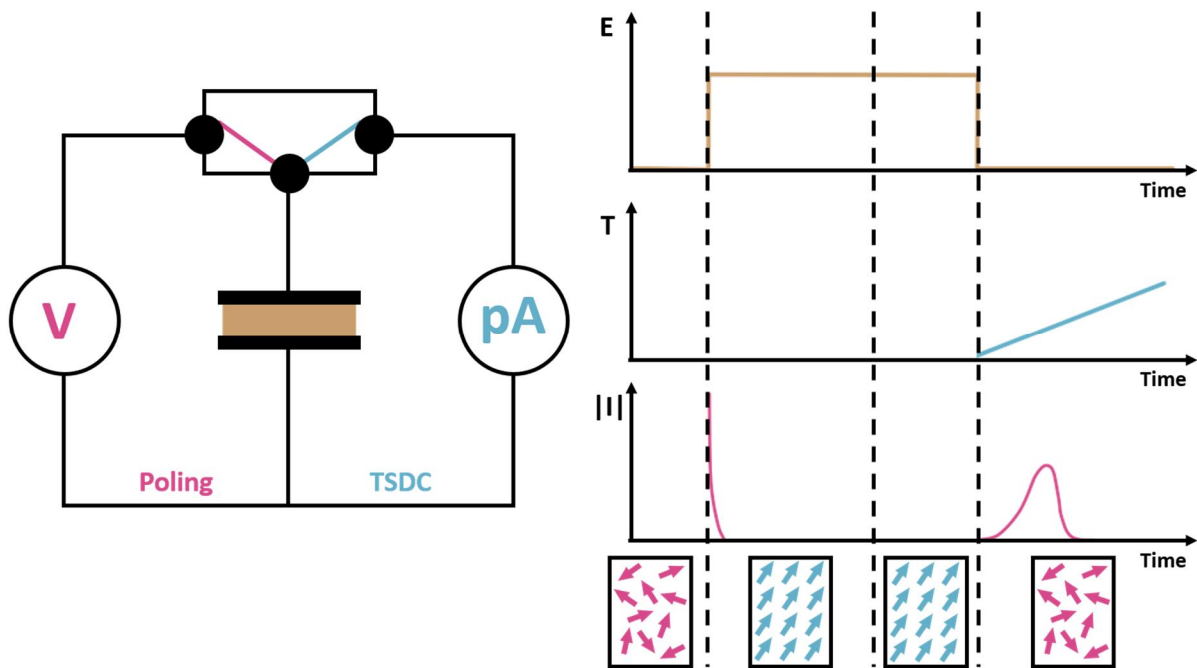
Figure 14. System scheme for poling and measurement of TSDC with profile of electric field (E), temperature (T) and current (I) in poling & TSDC measurement process.

3.2.6. Piezoelectric constant

The piezoelectric constant (d_{33}) was measured by quasi-static method using d_{33} meter (YE2730A, Sinocera, Yangju ,China) at frequency of 110Hz.

4. Experimental results & Discussion

4.1. X-ray diffraction

X-ray diffraction pattern of powder of single crystal at room temperature was obtained for confirming crystallographic structure of crystal. **Figure 15 (a)** shows the XRD patterns of crushed single crystals and indicates a perovskite phase. The (211) reflection is split indicating rhombohedral structure of Mn-doped PMN-PT (see **Figure 15 (b)**).
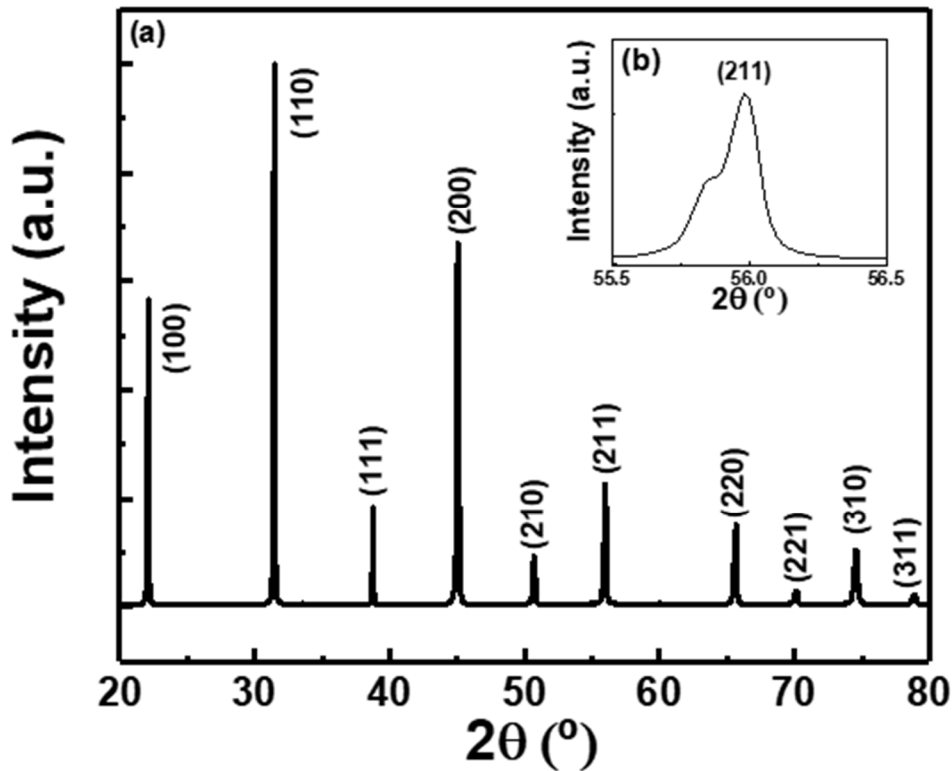
Figure 15. **(a)** Powder XRD patterns of the grind Mn-doped PMN-PT crystals, indicating a pure perovskite structure. **(b)** (211) peak indicating rhombohedral symmetry.

4.2. X-ray photoelectron spectroscopy

For confirming oxidation states of Mn, X-ray photoelectron spectroscopy data was obtained. **Figure 16** gives the XPS spectrum in the binding energy range of 630-660 eV. The main peak can be separated to two peaks at 642eV and 644eV. The dominant peak indicates Mn^{3+} and minor one indicates Mn^{2+} state.
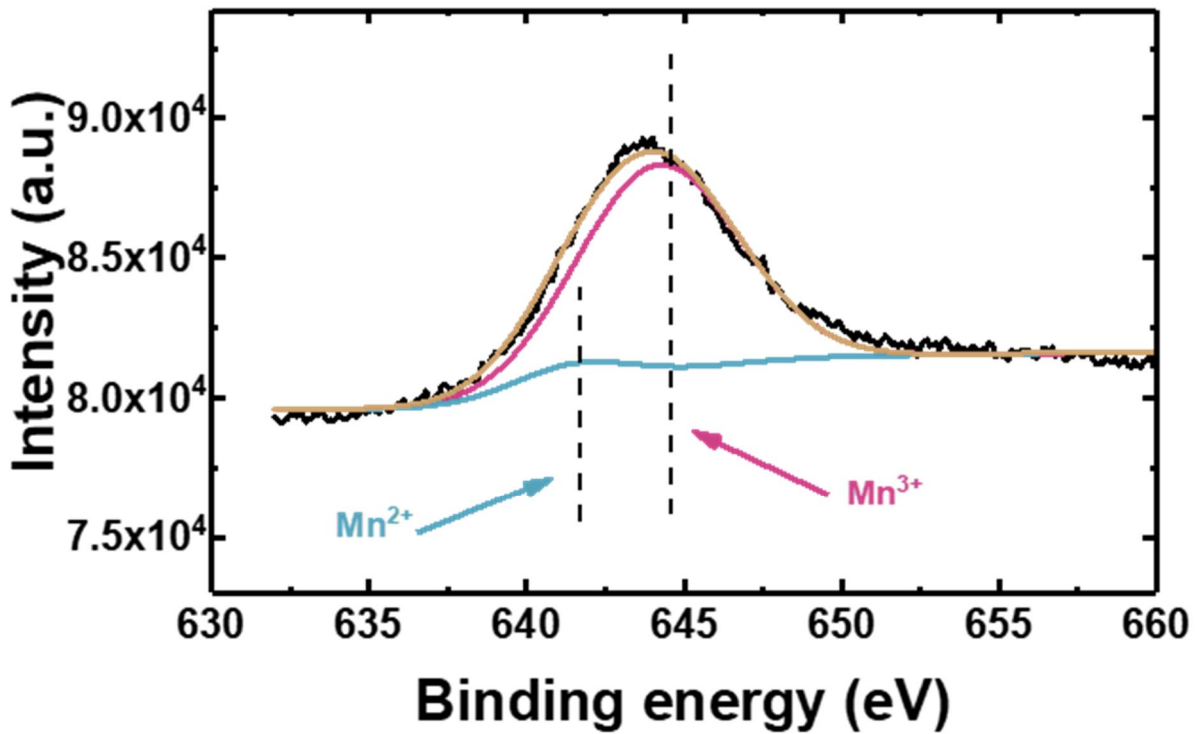
Figure 16. The XPS spectrum of Mn doped PMN-PT single crystals, showing the Mn^{2+} and Mn^{3+} ions in the crystal.

4.3. Electric field induced properties

Electric field induced properties of pure PMN-PT and Mn doped PMN-PT single crystals (Polarization-field (P-E) hysteresis loop) is given in **Figure 17**. Both curves have a common curve of ferroelectric single crystals. However, compared to pure PMN-PT, the P-E curve of Mn doped PMN-PT has asymmetric appearance. The cause of these asymmetric P-E hysteresis loop is known as defect which occurs domain pinning effects.[25] The positive coercive field (E_{c+}) and negative coercive field (E_{c-}) of Mn doped PMN-PT crystal are 0.kV/mm and -0 respectively. And internal bias field (E_i) is calculated to 0.139kV/mm by following **equation (11)**.

$$E_i = (E_{c+} + E_{c-})/2 \qquad\qquad (11)$$
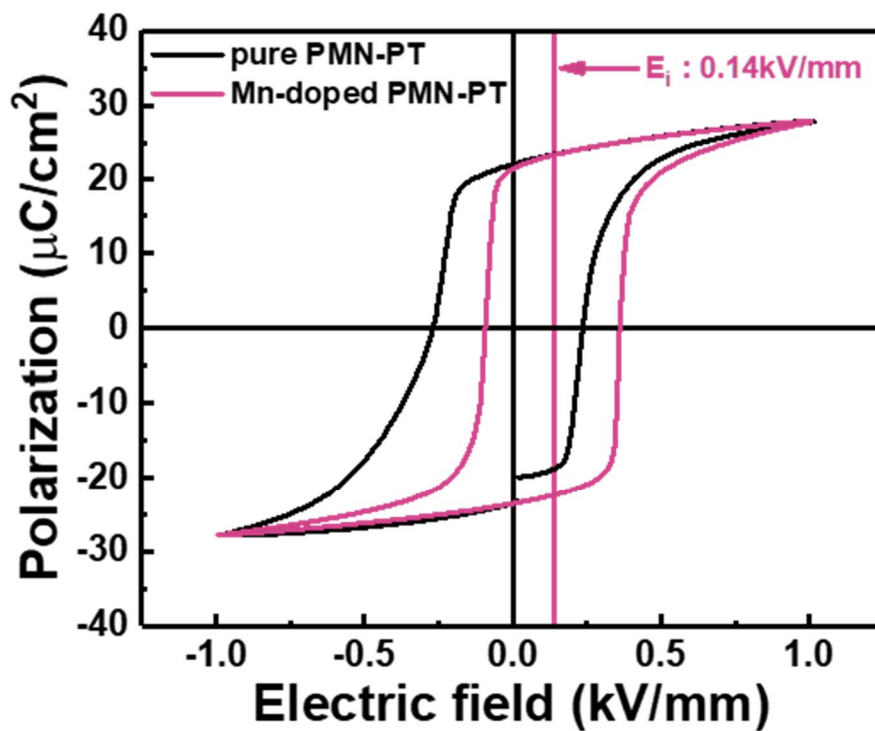
Figure 17. Ferroelectric hysteresis loops of pure PMN-PT single crystal and Mn-doped PMN-PT single crystal with asymmetric appearance.

Figure 18 shows temperature dependence of E_{c+}, E_{c-} and E_i. As the temperature increases, the difference between E_{c+} and E_{c-} decreases and E_{c-} gets positive value above 140 °C. The internal bias field remains up to Curie temperature (Tc) of Mn-doped PMN-PT single crystals (= 150 °C) and above Tc, E_i begin to decline. The remaining internal bias field may affect the formation and alignment of ferroelectric domains during cooling.
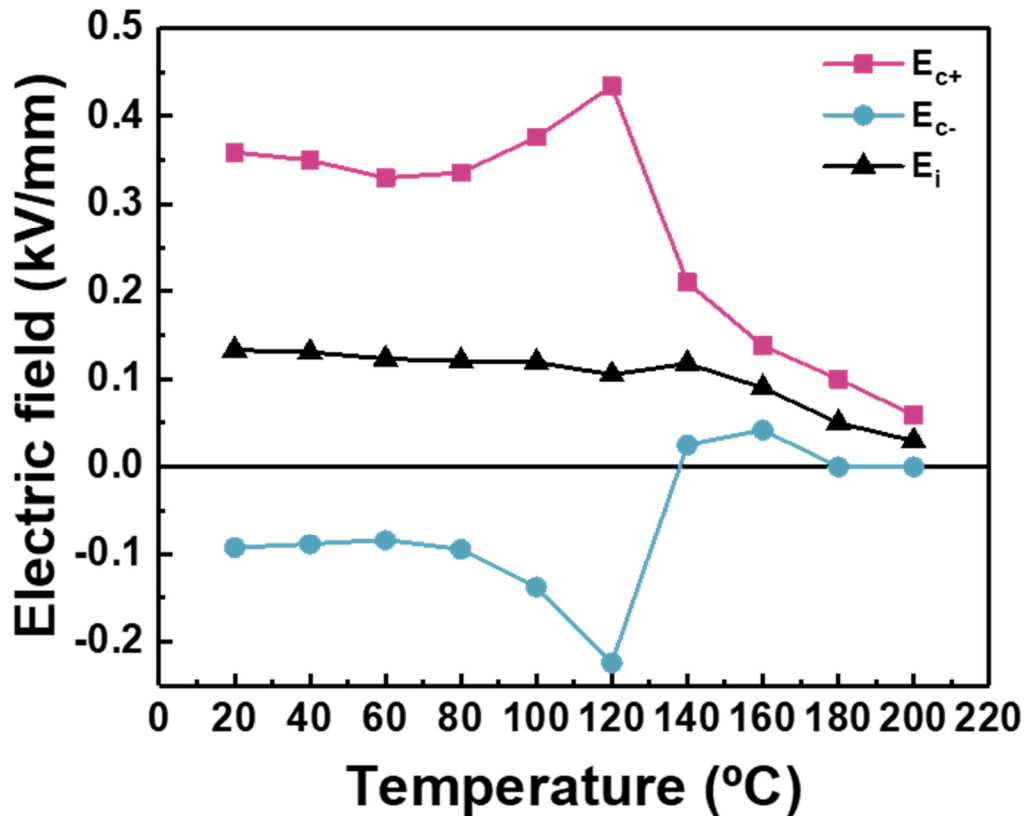
Figure 18. Temperature dependence of coercive field (E_{c+} & E_{c-}) and internal bias field (E_i) of Mn-doped PMN-PT single crystal.

4.4. Temperature dependence of dielectric permittivity and

dielectric loss

The temperature dependences of the dielectric permittivity and dielectric loss of pure PMN-PT single crystals and Mn doped PMN-PT is shown in **Figure 19**. The dielectric permittivity of the Mn-doped PMN-PT is 4730 which is smaller than that of the pure PMN-PT single crystals. The rhombohedral to tetragonal phase transition temperature (T_{R-T} ,105ºC) and Tc (151ºC) of increased compare to T_{R-T} (90ºC) and Tc (120ºC) of pure PMN-PT. The depression of dielectric permittivity and increased T_{R-T} and Tc are typical phenomena caused by hardening effect.
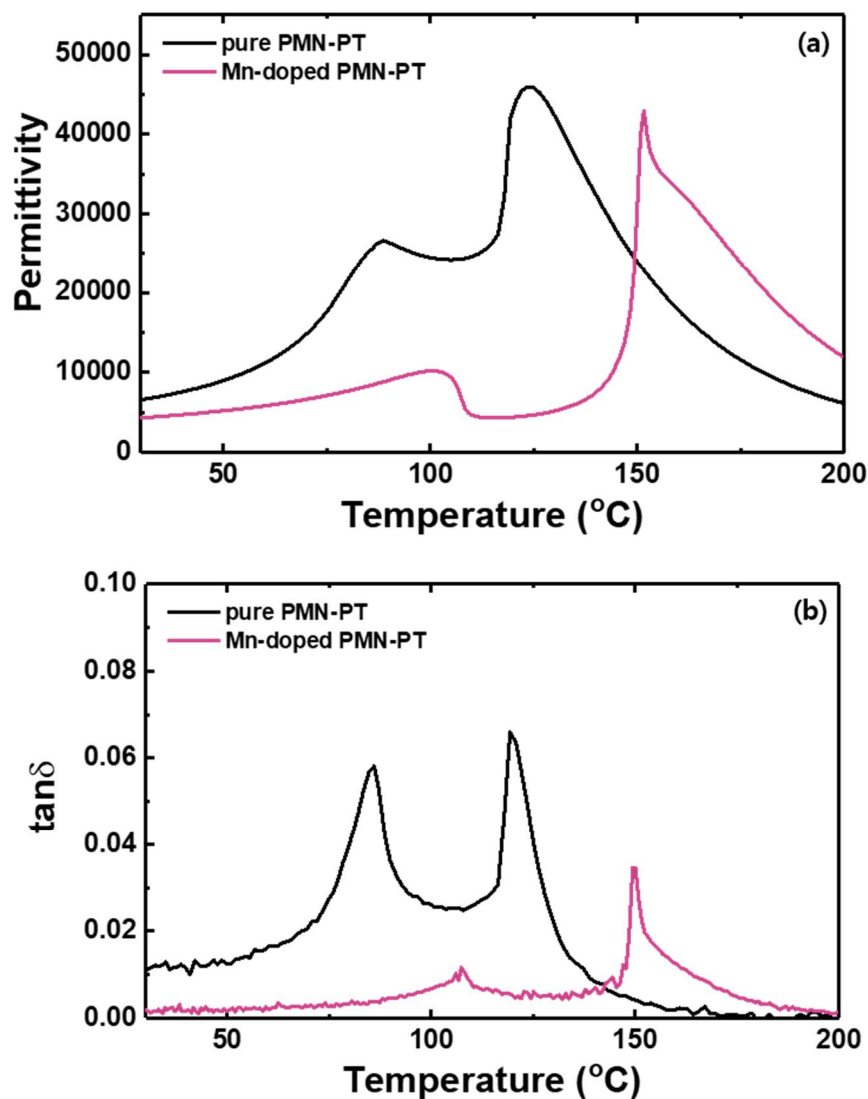
Figure 19. Temperature dependence of **(a)** dielectric permittivity at 1kHz and **(b)** dielectric loss at 1kHz of pure & Mn-doped PMN-PT single crystals.

4.5. Thermally stimulated depolarization current

Thermally stimulated depolarization current data of pure & Mn-doped PMN-PT is given in **Figure 20**. In this figure, when depolarization occur, the current peak points upward. In case of pure PMN-PT, only depolarization peak is observed at T_{R-T} and Tc. However, there is no changes of current in the cooling process in TSDC data of pure PMN-PT. (See **Figure 20 (a)**.) In **Figure 20 (b)**, there are also two peaks in heating process for Mn-doped PMN-PT at T_{R-T} and Tc. However, the peak of T_{R-T} points downward unlike that of pure PMN-PT. Interestingly, there are two peaks in cooling process of Mn-doped PMN-PT single crystals. Near Tc, there is spontaneous poling a.k.a. self-poling. The reason for this self-poling is the remained internal bias field above Tc which is mentioned before. Ferroelectric domains are more easily aligned at high temperature. So internal bias field can make spontaneous polarization of Mn-doped PMN-PT single crystals.
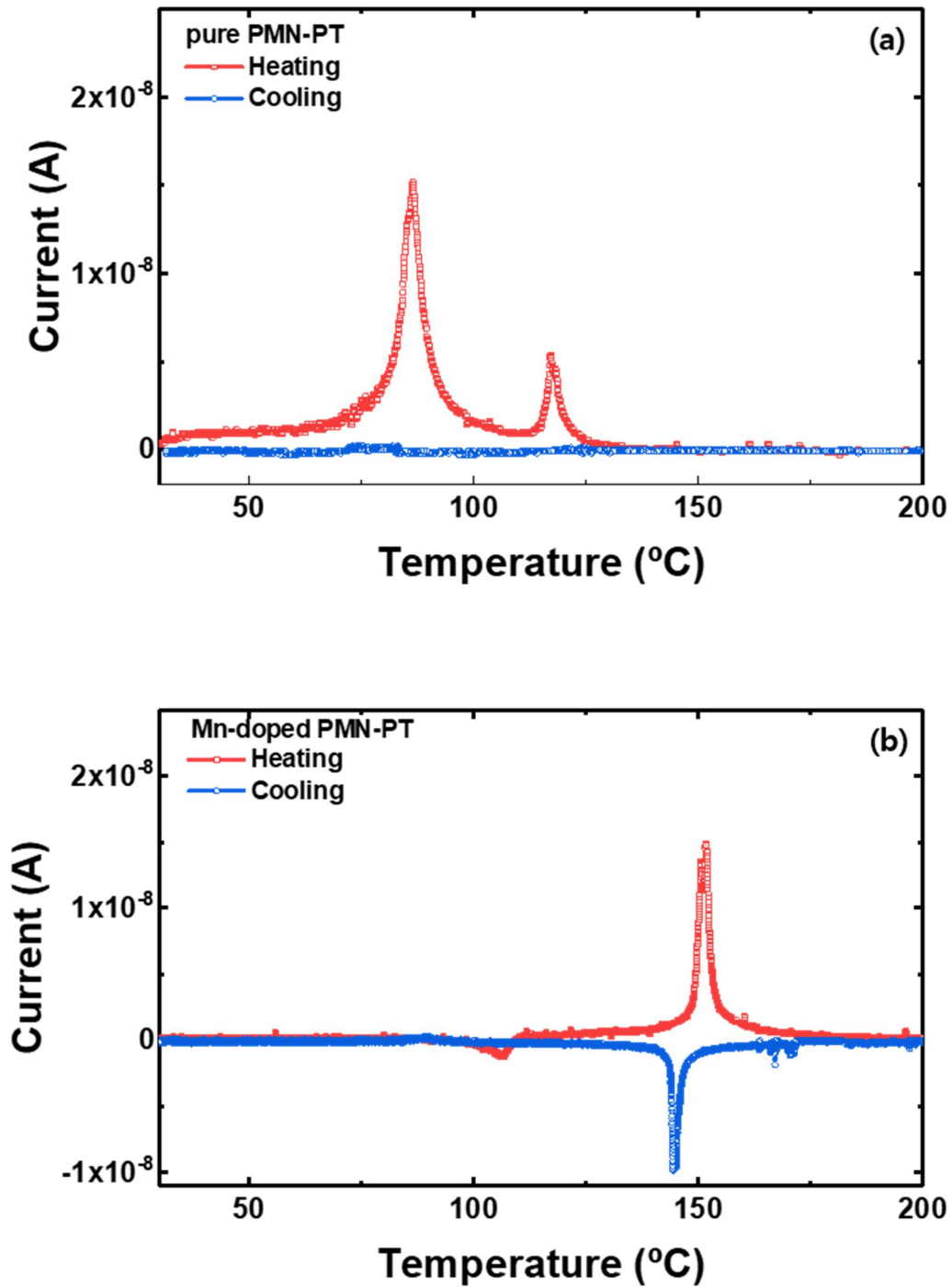
Figure 20. Thermally stimulated depolarization current data of (a) pure PMN-PT (b) Mn-doped PMN-PT

Figure 21 describes temperature dependence of polarization of Mn-doped PMN-PT single crystals. The polarization is calculated by integration of depolarization and polarization current. Near Tc, polarization decreases dramatically in heating process and increase in cooling process. But near T_{R-T}, polarization phenomena show opposite tendency to those of Tc in both heating and cooling process. For explaining phenomena near T_{R-T}, additional studies are needed.
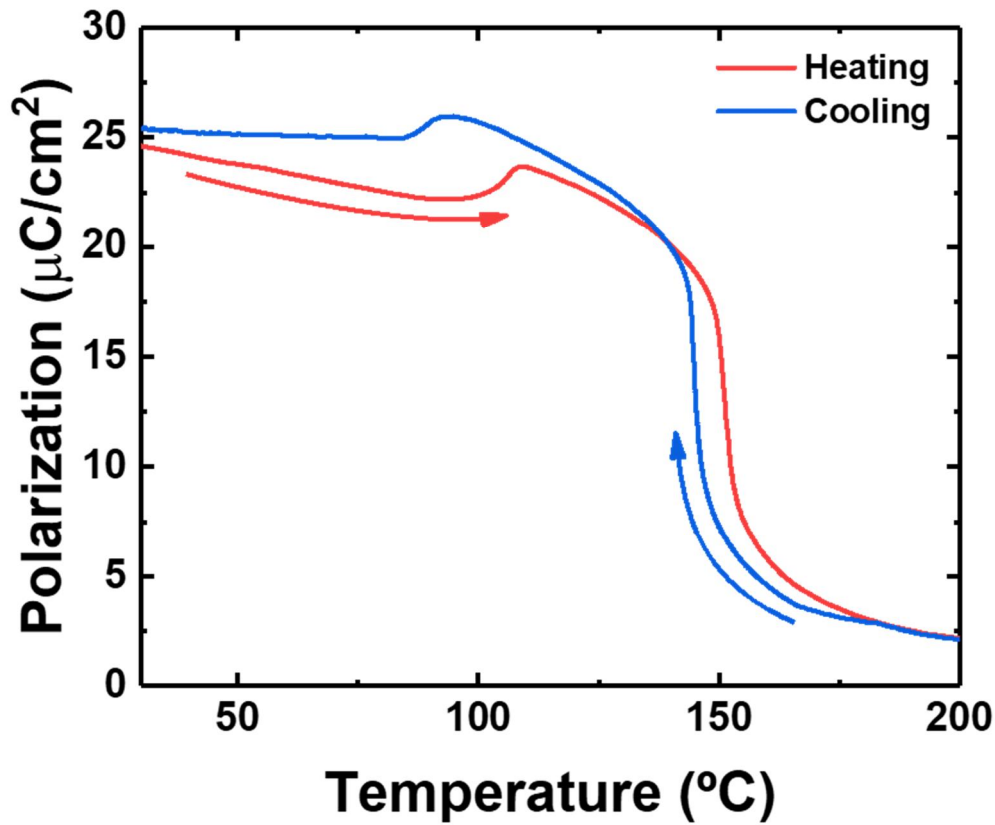
Figure 21. Temperature dependence of polarization of Mn-doped PMN-PT single crystals.

4.6. Quenching for inhibiting self-polarization

To get ferroelectric virgin state of Mn-doped PMN-PT single crystals, air quenching from 300°C to RT is performed. Compared to furnace cooled crystals, dielectric permittivity and piezoelectric constant of quenched crystal decreased. (see **Figure 22**) The air quenching polarization was able to reduce spontaneous polarization. However, piezoelectric response of Mn-doped PMN-PT single crystal was not completely eliminated.

**Furnace cooling**
20°C
Piezoelectric constant : 1060pC/N
Dielectric permittivity (1kHz) : 3650

Air quenching
20°C
Piezoelectric constant : 10 – 50pC/N
Dielectric permittivity (1kHz) : 1710
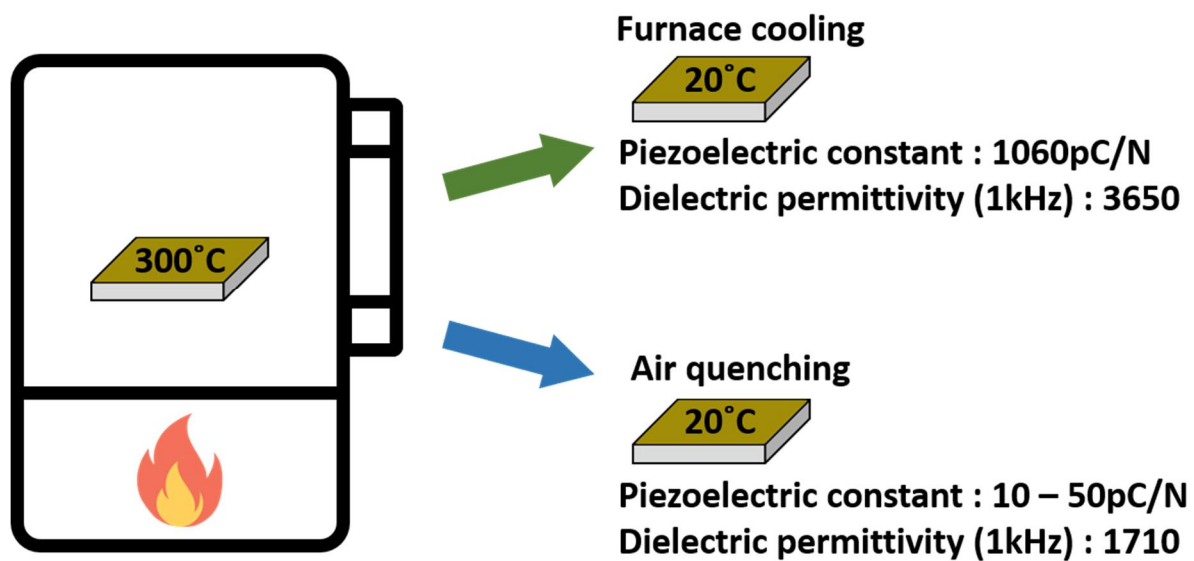
Figure 22. Comparison of piezoelectric constant at 20°C and dielectric permittivity at 1kHz, 20°C of furnace cooled & air quenched Mn-doped PMN-PT.

Figure 23 describes TSDC and temperature dependence of permittivity data of quenched Mn-doped PMN-PT crystals and **Figure 24** shows temperature dependence of polarization of quenched Mn-doped PMN-PT on heating process. Near T_{R-T}, same current peak can be observed same as self-poled crystals and polarization increases. But in case of dielectric permittivity, there is no peak at T_{R-T} but only plateau (or shoulder) in the range of 120°C -140°C. Unlike self-poled crystal, another downward peak appears before depolarization current peak. The polarization also increases just below Tc and decreases rapidly afterwards. In case of quenched crystals, both poling and depoling can be observed near Tc.

Figure 23. TSDC and temperature dependence of dielectric permittivity at 1kHz quenched Mn-doped PMN-PT single crystals.

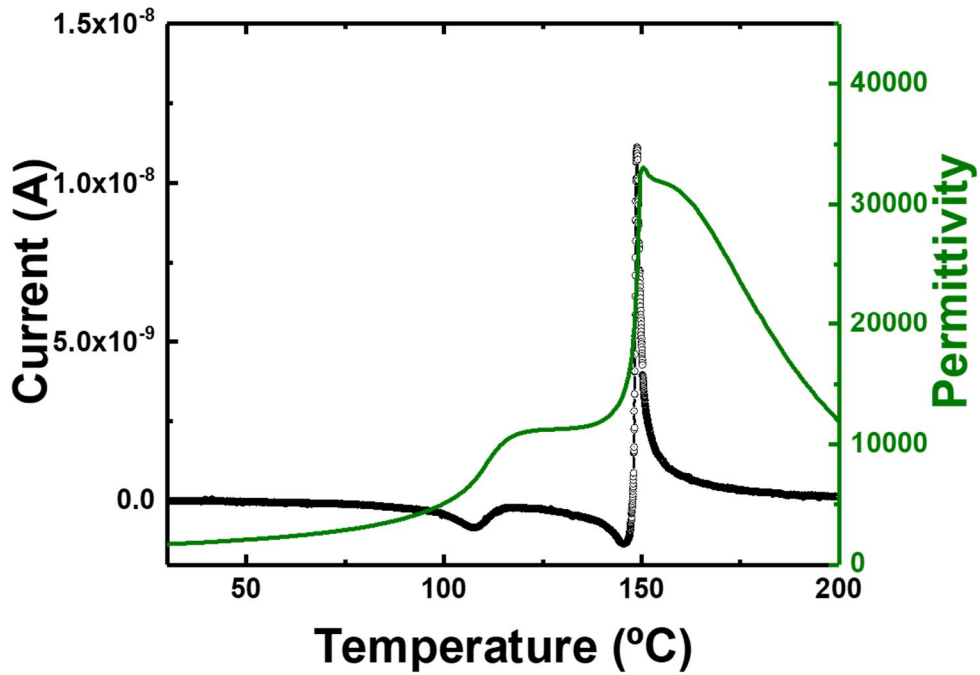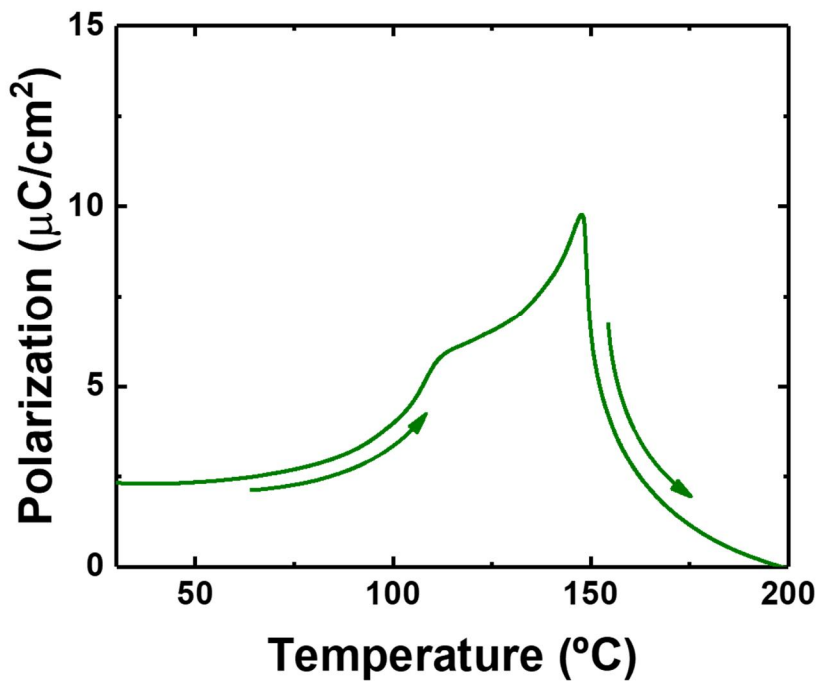**Figure 24**. Temperature dependence of polarization of Quenched Mn-doped PMN-PT single crystals.

4.7. Dielectric and piezoelectric enhancement as function of temperature on Mn-doped PMN-PT single crystal

Quenched Mn-doped PMN-PT crystals were heated at different target temperature for investigating optimized temperature for self-poling effect. The target temperature was selected at 75°C below T_{R-T}, 125°C between T_{R-T} and Tc, and 175°C above Tc. When annealing temperature was 75°C, any polarization/depolarization currents of Mn-doped PMN-PT crystals were not observed (See **Figure 25 (a)**). In the **Figure 25 (b)**, current peaks can be observed near 100°C. Both current peaks indicate there was alignment of dipoles. In case of 175°C, same result with previous TSDC and temperature dependence of permittivity of Mn-doped PMN-PT crystals can be observed. Interestingly, there was polarization process near 100°C in **Figure 25 (b)**, but depolarization occurs near 100°C in **Figure 25 (c)**.

The enhanced dielectric permittivity and piezoelectric constant of quenched Mn-doped PMN-PT are shown in Table 3. when target temperature was 75°C, self-poling effect was not induced. Both of piezoelectric constant and dielectric permittivity were not improved at all. The piezoelectric constant and dielectric permittivity of crystals were slightly enhanced when the annealing temperature was 125°C. The piezoelectric constant and dielectric permittivity increased by 10 times and 52% respectively. The highest piezoelectric constant and dielectric permittivity can be obtained at which target temperature was 175°C. Self-poling effect perfectly induced near Tc as can be seen from **Figure 25 (c)** and **Table 3**. So annealing temperature for the optimized self-poled crystal should be above Tc = 150°C.
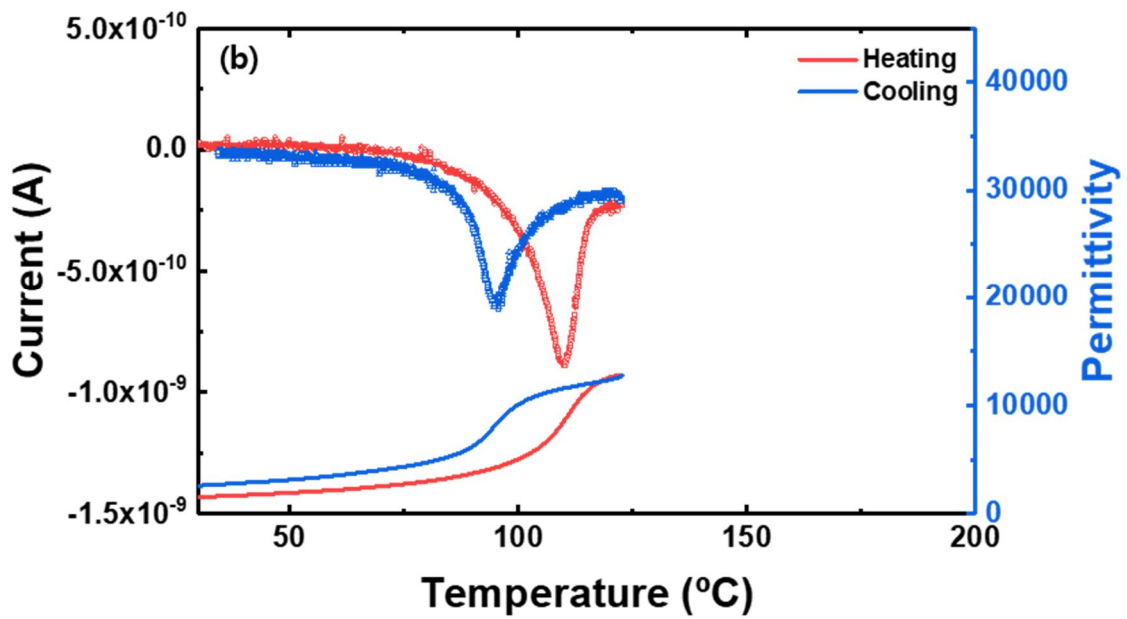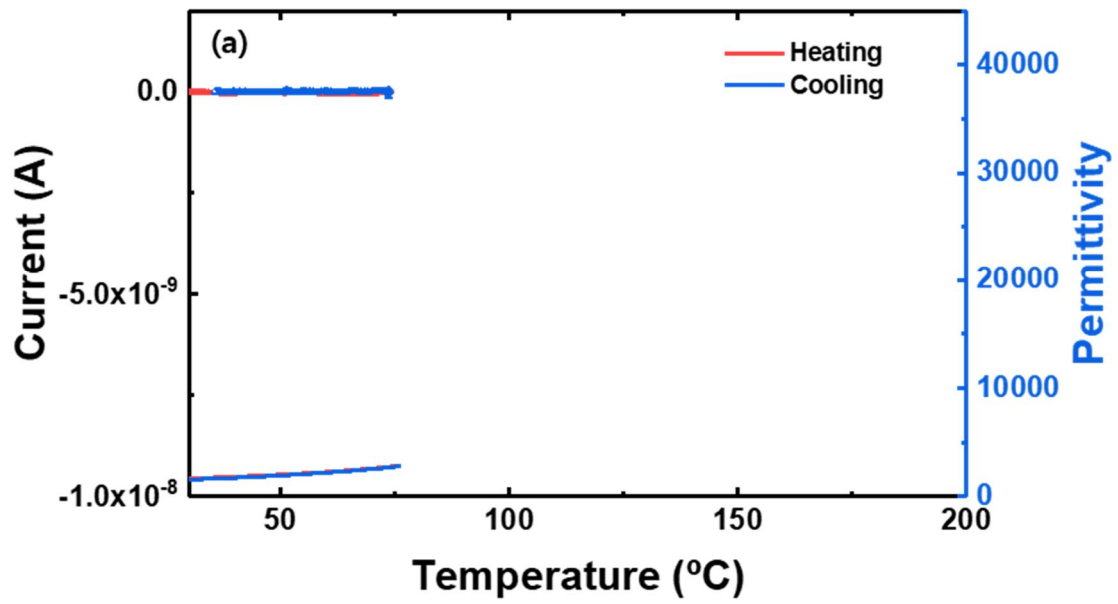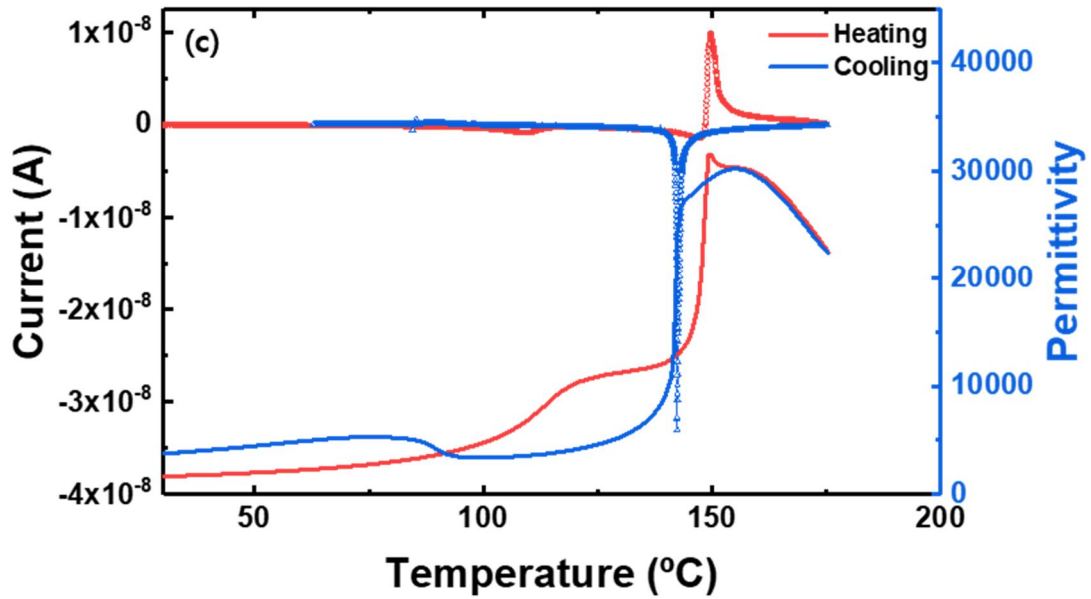
Figure 25. TSDC and temperature dependence at different target temperature (a) 75ºC ,(b) 125ºC ,(c) 175ºC.

Target temperature	Quenched	75ºC	125ºC	175ºC
Piezoelectric constant (20ºC)	10~50	10~50	240	1080
Dielectric permittivity (1kHz, 20ºC)	1710	1590	2610	3760

Table 3. Enhanced dielectric permittivity & piezoelectric constant with different annealing temperature.

4.8. Direct current poling on self-poled Mn-doped PMN-PT single crystals

To enhance the piezoelectric constant and dielectric permittivity, direct current poling(DCP) was performed on self-poled Mn-doped PMN-PT. **Figure 26** describes experimental scheme and **Table 4** shows the enhanced piezoelectric constant and dielectric permittivity of DC poled crystals.
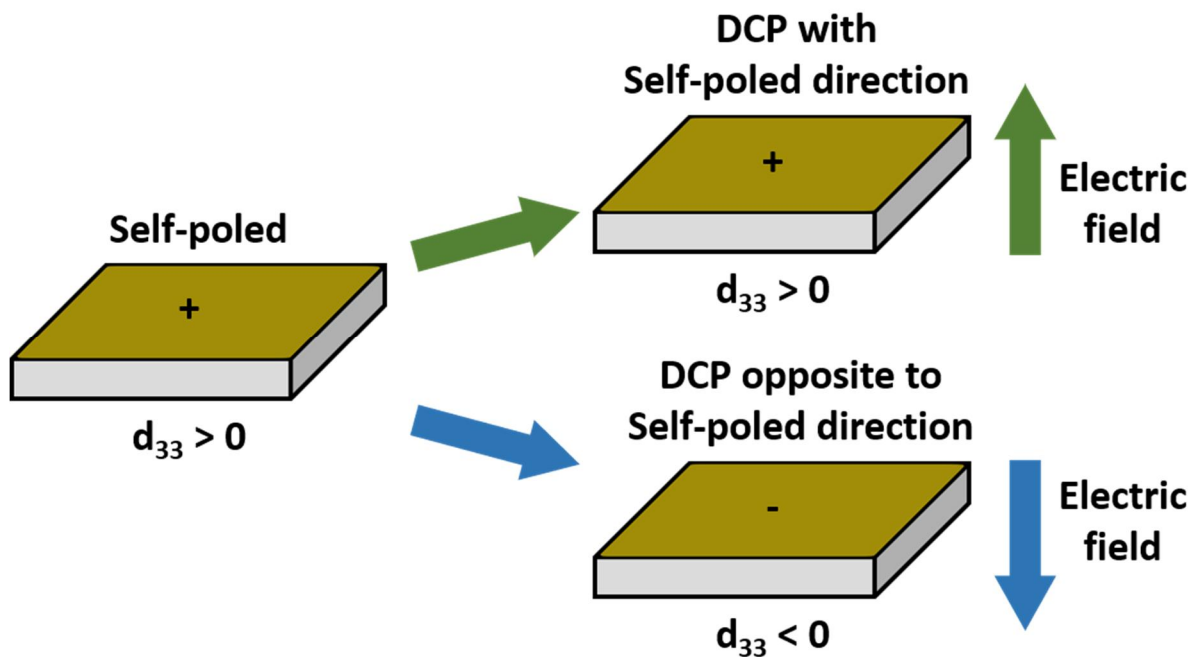
Figure 26. Experimental scheme of DCP on self-poled Mn-doped PMN-PT single crystals with different direction.

Poling state	Quenched	Self-poled	DCP with self-poled direction	DCP opposite to self-poled direction
Piezoelectric constant (20ºC)	10~50	1080	1200	-1350
Dielectric permittivity (1kHz, 20ºC)	1710	3760	4190	4960

Table 4. Enhanced dielectric permittivity & piezoelectric constant with different poling state

Firstly, self-poling was always in the same direction although crystal was quenched. That means, the defect dipoles, which can be the reason why self-poling occur, stick their own direction regardless of any heating or electric treatment. When the direction of DCP was same as that of self-poling, the piezoelectric constant and dielectric permittivity was slightly improved compared to those of self-poled crystals.

However, the piezoelectric and dielectric performances of DC-poled crystals with opposite direction was quite higher than self-poled crystals. This can be seen as having a similar effect of alternating current poling (ACP), given that two opposite poling directions have been processed. **Figure 27** shows the temperature dependence of dielectric permittivity of Mn-doped PMN-PT poled with different poling conditions. Same as reported temperature dependence of dielectric permittivity of AC-poled PMN-PT single crystals[24], there is additional peak of permittivity. And overall dielectric permittivity increased compared to DC-poled with same direction of self-poling.
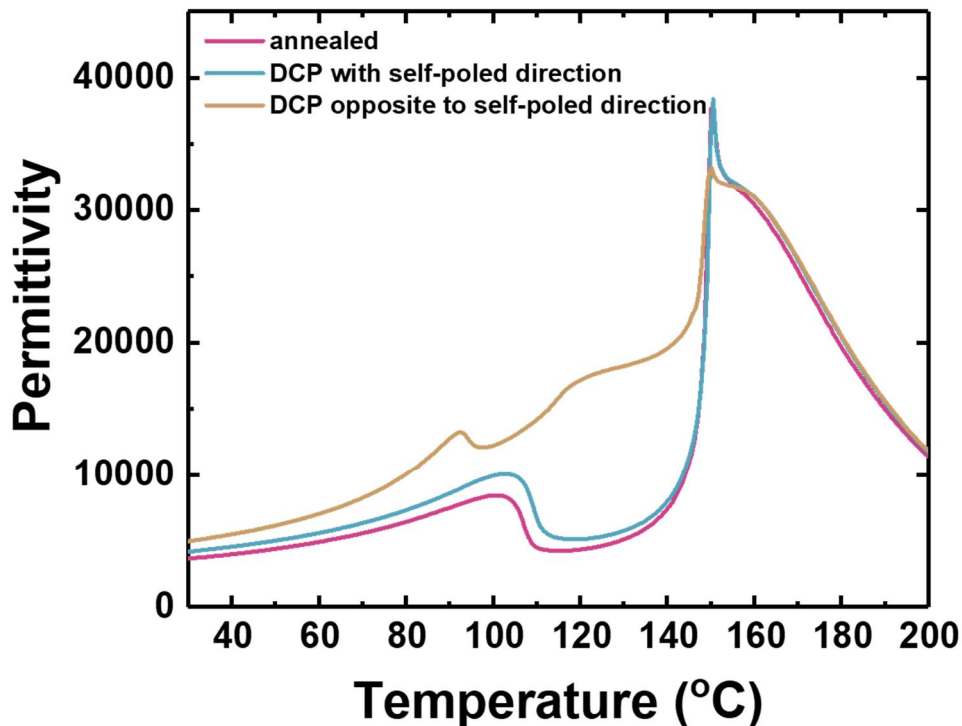

Figure 27. Temperature dependence of dielectric permittivity of Mn-doped PMN-PT poled with different poling condition.

5. Conclusion

  In this work, self-poling effect of Mn-doped PMN-PT single crystal was discussed. The Mn-doped PMN-PT ferroelectric single crystals was synthesized by SSCG method. The rhombohedral perovskite structure of single crystal was confirmed by powder XRD. The self-poling is induced by the defect dipoles which can be induced by Mn dopants which have multi-valence states supported by XPS. The internal bias field which remains even above Curie temperature (T_c) can be observed by temperature dependence of polarization-electric field measurement. The poling process can be observed by TSDC measurement. TSDC shows self-poling current peak even in cooling process a.k.a. not thermally stimulated. Near T_{R-T}, there was weak depoling current peak, but mechanism of current peak near T_{R-T} needs more studies. The temperature dependence of enhanced piezoelectric and dielectric properties was obtained for checking optimized annealing temperature for self-poling effect. To gain perfectly self-poled state, Mn-doped PMN-PT single crystal should be cooled from above 150ºC, T_c. These results show the piezoelectric properties of ferroelectric single crystal can be induced without poling process but only Mn-modified system.

  Additionally, self-poling effect on Mn-doped PMN-PT can be inhibited by quenching. However, there was remained weak piezoelectric response after quenching. The self-poling effect was time-dependent process. Self-poling effects induced by defect dipoles memorize their own poling directions. Opposite DC-poling process can enhance the piezoelectric and dielectric properties and it is similar to AC-poling. The direction of additional poling on self-poled piezoelectric crystals is important to enhance the piezoelectric and dielectric properties of single crystals which have self-poling effect.

6. References

[1] I. P. Kaminow, *Principles and applications of ferroelectrics and related materials*, vol. 66, no. 10. Oxford: Oxford University Press, 2008.

[2] J. Moulson, A and Herbert, *Electroceramics: Materials, Properties, Applications.*, 2 ed. Chichester, England: Wiley, 2003.

[3] W. J. Merz, "The electric and optical behavior of BaTiO3 single-domain crystals," *Phys. Rev.*, vol. 76, no. 8, pp. 1221–1225, Oct. 1949.

[4] B. Jaffe, W. Cook, and H. Jaffe, *Piezoelectric Ceramic*, vol. 3. 1971.

[5] P. Chandra and P. Littlewood, "A Landau Primer for Ferroelectrics," in *Topics in Applied Physics*, vol. 105, 2007, pp. 69–116.

[6] D. Lupascu *et al.*, "Mechanical Properties of Ferro-Piezoceramics," in *Springer Series in Materials Science*, vol. 140, 2011, pp. 469–542.

[7] D. Damjanovic, "Ferroelectric, Dielectric and Piezoelectric Properties of Ferroelectric Thin Films and Ceramics," *Reports Prog. Phys.*, vol. 61, Sep. 1998.

[8] H. T. Oh, J. Y. Lee, and H. Y. Lee, "Mn-modified PMN-PZT [Pb(Mg1/3Nb2/3)O3-Pb(Zr,Ti)O3] single crystals for high power piezoelectric transducers," *J. Korean Ceram. Soc.*, vol. 54, no. 2, pp. 150–157, Mar. 2017.

[9] J. Kuwata, K. Uchino, and S. Nomura, "Dielectric and piezoelectric properties of 0.91pb(zn1/3nb2/3)o3-0.09pbtio3 single crystals," *Jpn. J. Appl. Phys.*, vol. 21, no. 9R, pp. 1298–1302, Sep. 1982.

[10] S. E. Park and T. R. Shrout, "Ultrahigh strain and piezoelectric behavior in relaxor based ferroelectric single crystals," *J. Appl. Phys.*, vol. 82, no. 4, pp. 1804–1811, Aug. 1997.

[11] S. Zhang, S.-M. Lee, D.-H. Kim, H.-Y. Lee, and T. R. Shrout, "Characterization of Mn-modified Pb(Mg1∕3Nb2∕3)O3–PbZrO3–PbTiO3 single crystals for high power broad bandwidth transducers," *Appl. Phys. Lett.*, vol. 93, no. 12, p. 122908, Sep. 2008.

[12] Z. G. Ye, "Handbook of Advanced Dielectric, Piezoelectric and Ferroelectric Materials: Synthesis, Properties and Applications," *Handbook of Advanced Dielectric, Piezoelectric and Ferroelectric Materials: Synthesis, Properties and Applications*. Burlington :, pp. 1–1060, 2008.

[13] S. Zhang, L. Lebrun, D. Y. Jeong, C. A. Randall, Q. Zhang, and T. R. Shrout, "Growth

and characterization of Fe-doped Pb(Zn1/3Nb2/3)O3-PbTiO3 single crystals," *J. Appl. Phys.*, vol. 93, no. 11, pp. 9257–9262, May 2003.

[14]   S. Priya and K. Uchino, "High power resonance characteristics and dielectric properties of co-substituted 0.92Pb(Zn1/3Nb2/3)O3-0.08PbTiO3 single crystal," *Japanese Journal of Applied Physics, Part 1: Regular Papers and Short Notes and Review Papers*, vol. 42, no. 2 A. Tokyo :, pp. 531–534, 2003.

[15]   S. Priya, K. Uchino, and D. Viehland, "Crystal growth and piezoelectric properties of Mn-substituted Pb(Zn1/3Nb2/3)O3 single crystal," *Japanese Journal of Applied Physics, Part 2: Letters*, vol. 40, no. 10 A. Tokyo :, pp. L1044–L1047, 2001.

[16]   S. Zhang, L. Lebrun, C. A. Randall, and T. R. Shrout, "Growth and electrical properties of (Mn,F) co-doped 0.92Pb(Zn 1/3Nb2/3)O3-0.08PbTiO3 single crystal," *J. Cryst. Growth*, vol. 267, no. 1–2, pp. 204–212, 2004.

[17]   S. Priya, K. Uchino, and D. Viehland, "Fe-substituted 0.92Pb(Zn1/3Nb2/3)O 3-0.08PbTiO3 single crystals: A 'hard' piezocrystal," *Appl. Phys. Lett.*, vol. 81, no. 13, pp. 2430–2432, Sep. 2002.

[18]   D. Kobor, L. Lebrun, G. Sébald, and D. Guyomar, "Characterization of pure and substituted 0.955Pb(Zn1/3Nb 2/3)O3-0.045PbTiO3," *J. Cryst. Growth*, vol. 275, no. 3–4, pp. 580–588, 2005.

[19]   Y. Tang *et al.*, "Mn-doped 0.71Pb (Mg 1/3 Nb 2/3)O 3 -0. 29PbTiO 3 pyroelectric crystals for uncooled infrared focal plane arrays applications," *Appl. Phys. Lett.*, vol. 89, no. 16, p. 162906, Oct. 2006.

[20]   C. S. Tu, F. T. Wang, R. R. Chien, V. H. Schmidt, C. M. Hung, and C. T. Tseng, "Dielectric and photovoltaic phenomena in tungsten-doped Pb(Mg 1/3 Nb 2/3) 1-xTi xO 3crystal," *Appl. Phys. Lett.*, vol. 88, no. 3, pp. 1–3, Jan. 2006.

[21]   Y. Sato *et al.*, "Photorefractive effect and photochromism in the Fe-doped relaxor ferroelectric crystal Pb(Zn1/3Nb2/3)O3- PbTiO3," *J. Appl. Phys.*, vol. 96, no. 9, pp. 4852–4855, Oct. 2004.

[22]   Y. Yamashita, "Piezoelectric transducer, ultrasonic probe, and piezoelectric transducer manufacturing method." 2015.

[23]   J. Xu *et al.*, "Piezoelectric performance enhancement of Pb(Mg 1/3 Nb 2/3)O 3 -0.25PbTiO 3 crystals by alternating current polarization for ultrasonic transducer," *Appl. Phys. Lett.*, vol. 112, no. 18, p. 182901, Apr. 2018.

[24] W. Y. Chang *et al.*, "Dielectric and piezoelectric properties of 0.7 Pb(Mg 1/3 Nb 2/3)O 3 -0.3 PbTiO 3 single crystal poled using alternating current," *Materials Research Letters*, vol. 6, no. 10. Abingdon, Oxfordshire, UK :, pp. 537–544, 2018.

[25] B. S. Li, G. R. Li, Q. R. Yin, Z. G. Zhu, A. L. Ding, and W. W. Cao, "Pinning and depinning mechanism of defect dipoles in PMnN-PZT ceramics," *Journal of Physics D: Applied Physics*, vol. 38, no. 8. London :, pp. 1107–1111, 2005.